Strong coupling from $e^+e^- \to$ hadrons below charm

Diogo Boito,[1] Maarten Golterman,[2,3] Alexander Keshavarzi,[4,*] Kim Maltman,[5,6] Daisuke Nomura,[7] Santiago Peris,[2] and Thomas Teubner[4]

[1]*Instituto de Física de São Carlos, Universidade de São Paulo, CP 369, 13570-970 São Carlos, SP, Brazil*
[2]*Department of Physics and IFAE-BIST, Universitat Autònoma de Barcelona, E-08193 Bellaterra, Barcelona, Spain*
[3]*Department of Physics and Astronomy, San Francisco State University, San Francisco, California 94132, USA*
[4]*Department of Mathematical Sciences, University of Liverpool, Liverpool L69 3BX, United Kingdom*
[5]*Department of Mathematics and Statistics, York University, Toronto, Ontario M3J 1P3, Canada*
[6]*CSSM, University of Adelaide, Adelaide, South Australia 5005, Australia*
[7]*KEK Theory Center, Tsukuba, Ibaraki 305-0801, Japan*

(Received 29 May 2018; published 31 October 2018)

We use a new compilation of the hadronic R-ratio from available data for the process $e^+e^- \to$ hadrons to determine the strong coupling, α_s. We make use of all data for the R-ratio from threshold to a center-of-mass energy of 2 GeV by employing finite-energy sum rules. Data above 2 GeV, for which at present far fewer high-precision experimental data are available, do not provide much additional constraint but are fully consistent with the values for α_s we obtain. Quoting our results at the τ mass to facilitate comparison to the results obtained from analogous analyses of hadronic τ-decay data, we find $\alpha_s(m_\tau^2) = 0.298 \pm 0.016 \pm 0.006$ in fixed-order perturbation theory, and $\alpha_s(m_\tau^2) = 0.304 \pm 0.018 \pm 0.006$ in contour-improved perturbation theory, where the first error is statistical, and the second error reflects our estimate of various systematic effects. These values are in good agreement with a recent determination from the OPAL and ALEPH data for hadronic τ decays.

DOI: 10.1103/PhysRevD.98.074030

I. INTRODUCTION

There are many hadronic quantities from which the strong coupling, $\alpha_s(s)$, can be extracted, at many different energy scales $E = \sqrt{s}$, as long as s is large enough that QCD perturbation theory can be expected to apply. The range of scales employed in such determinations ranges from above the Z mass, where nonperturbative effects are negligible, down to the τ mass, where these effects, although subdominant, must be taken into account carefully in an accurate extraction of α_s. Not all of these determinations lead to values for α_s (quoted, for instance, in the 5-flavor, $\overline{\text{MS}}$ scheme at the Z mass) that are competitive when comparing the errors.[1] Nevertheless, determinations over a wide range of scales are interesting, because they directly test the running of the coupling predicted by QCD. As such, it is interesting to consider determinations of α_s at scales as low as the τ mass.

Some years ago, a calculation of the five-loop contribution to the Adler function [2] revived interest in the determination of α_s from nonstrange hadronic τ decays; for recent work see Refs. [3–12]. The results of these efforts have been controversial,[2] because it is difficult to disentangle nonperturbative contributions to the spectral functions extracted from hadronic τ decays, and, in fact, it is not obvious that this can be done in a completely satisfactory way. Moreover, it is difficult to make progress in the context of hadronic τ decays, because the τ mass puts a limit on the scales that can be probed within this approach.

It would thus be interesting to apply and test the same techniques in a similar setting where no such limit exists. This leads us to consider, instead of τ decays, the R-ratio $R(s)$, measured in the process $e^+e^- \to$ hadrons(γ), which is directly proportional to the electromagnetic (EM) QCD vector spectral function.[3] The same technology used in extracting α_s from the nonstrange, $I = 1$, vector and axial

*Present address: University of Mississippi. aikeshav@olemiss.edu

[1]For a recent review, see Ref. [1].

[2]See, in particular, Refs. [11,12] for a clear account of the controversy.

[3]The symbol (γ) indicates that the hadronic final state is inclusive of final-state radiation.

spectral functions measured in hadronic τ decays can also be used to extract α_s from the EM spectral function. The technology used in τ decays, which we apply here to $R(s)$ instead, is that of finite-energy sum rules (FESRs) [13–15].

The idea of comparing the predictions from QCD perturbation theory with $R(s)$ at large enough s is an old and obvious one. However, the extraction of $\alpha_s(s)$ from $R(s)$ at a single value of s leads to a very large uncertainty, which makes the resulting α_s compatible with other extractions, but uninteresting as a source of precise information about the coupling.[4] The use of FESRs, instead, allows us to make use of all data for $R(s)$ from threshold to some $s = s_0$, to extract α_s with a much higher precision than can be obtained from a "local" determination at the scale $s = s_0$. The reason a FESR determination is expected to be more precise is that, rather than relying only on a single local $R(s)$ result, FESRs employ weighted integrals over the experimental spectral distribution for s running from threshold to some upper limit s_0. Since the experimental data are more precise at lower s, the weighted spectral integrals for s_0 in the region where $R(s)$ starts to behave perturbatively are typically much more precise than are the values of $R(s)$ in the same region. The associated FESR determinations of α_s are thus also expected to be much more precise than those obtained by matching the perturbative expression for $R(s)$ to the spectral data directly. As we will see, a new compilation of $R(s)$ combining all available experimental electroproduction cross-section results [19] makes it possible to determine α_s at scales s_0 for $m_\tau^2 \lesssim s_0 \leq 4$ GeV^2 with an error small enough to make the comparison with other determinations of α_s interesting.[5] Moreover, we expect that future, more precise data for $R(s)$ will allow us to improve this determination of α_s, because at present the errors turn out to be dominated by those coming from the experimental errors on $R(s)$.[6]

As this paper will show, it is the data for the FESR integrals over $R(s)$ up to s_0 for values between $s_0 \approx m_\tau^2$ and $s_0 = 4$ GeV^2 that will contribute most to the accuracy with which we can determine α_s. Of course, data for $R(s)$ beyond 4 GeV^2 exist, but their accuracy is not yet sufficient to have a significant impact on the error in the determination of α_s. Although the τ mass plays no physical role in the current analysis, we will nonetheless quote our $n_f = 3$ flavor results for α_s at the scale $\mu = m_\tau$ in order to facilitate direct comparison to the results of the analogous τ-based analyses.

[4]See, for instance, Refs. [16–18] and, in particular, Table 3 in Ref. [17].

[5]Throughout this paper, we will actually use a version of the $R(s)$ data set of Ref. [19] slightly different from that employed in the evaluation of the leading order Hadronic Vacuum Polarization contribution to $(g-2)_\mu$ described in Ref. [19], for reasons explained in Sec. III A.

[6]Another recent compilation similar to, but independent of, the compilation of Ref. [19] can be found in Ref. [20].

The controversies that have plagued the determination of α_s from τ decays are primarily related to the need to model violations of quark-hadron duality associated with the clearly visible effects of hadronic resonances in the vector and axial spectral functions for $s \leq m_\tau^2$. At energies beyond the τ mass, duality violations are expected to decrease exponentially, making this a major motivation for considering the determination of α_s from $e^+e^- \to \text{hadrons}(\gamma)$. Indeed, while resonance effects are still present in the region $m_\tau^2 \leq s \leq 4$ GeV^2, it turns out that our central value for α_s from $R(s)$ is much less sensitive to the treatment of residual duality violations than was the case for τ-based analyses, with the modeling of these effects only needed as part of the analysis of systematic errors. It turns out that, given the current experimental errors on $R(s)$, our estimate for the systematic error due to duality violations is rather small.

This paper is organized as follows. In Sec. II, we provide a brief review of the necessary theory of FESRs. Contributions from perturbation theory (in the $\overline{\text{MS}}$ scheme) and the operator product expansion (OPE) are discussed in Sec. II B and the inclusion of electromagnetic corrections in the OPE (necessitated by the fact that the hadronic final states include photons) in Sec. II C. The contributions from duality violations are considered in some detail in Sec. II D. We describe and discuss the data in Sec. III, before turning to our analysis in Sec. IV. Section IV A contains our main fits to the data; Sec. IV B discusses systematic errors; and Sec. IV C contains our results, including a conversion to the five-flavor Z-mass scale. In Sec. IV D we compare these results to those obtained from an analogous τ-based analysis. Section V contains our conclusions.

II. THEORY

In this section, we review the FESR methodology, as applied to the case of the two-point function of the three-flavor EM current,

$$J_\mu^{\text{EM}} = \frac{2}{3}\bar{u}\gamma_\mu u - \frac{1}{3}\bar{d}\gamma_\mu d - \frac{1}{3}\bar{s}\gamma_\mu s = J_\mu^3 + \frac{1}{\sqrt{3}}J_\mu^8, \quad (2.1)$$

where the superscripts 3 and 8 label the neutral $I = 1$ and $I = 0$ members of the $SU(3)$ octet of three-flavor vector currents, respectively. The EM vacuum polarization $\Pi(q^2)$ is defined through[7]

$$\begin{aligned}\Pi_{\mu\nu}^{\text{EM}}(q) &= i\int d^4x e^{iqx}\langle 0|T\{J_\mu^{\text{EM}}(x)J_\nu^{\text{EM}}(0)\}|0\rangle, \\ &\equiv (q_\mu q_\nu - q^2 g_{\mu\nu})\Pi(q^2), \end{aligned} \quad (2.2)$$

[7]Note that, with this definition, in the isospin limit, the $I = 1$ part of $\Pi(q^2)$ has a normalization one-half that of the corresponding isovector flavor ud polarization encountered in the analysis of hadronic τ decays.

and the corresponding spectral function is obtained, as usual, from the imaginary part of $\Pi(q^2)$ as[8]

$$\rho(s) = \frac{1}{\pi}\mathrm{Im}\Pi(s) = \frac{1}{12\pi^2}R(s). \tag{2.3}$$

The second equality in Eq. (2.3) follows from the fact that the imaginary part of $\Pi(q^2)$ is directly related to the cross section for $e^+e^- \to$ hadrons, through the optical theorem. Here $R(s)$ is defined by

$$R(s) \equiv \frac{3s}{4\pi\alpha^2}\sigma_{e^+e^-\to\mathrm{hadrons}(\gamma)}(s) = \frac{\sigma_{e^+e^-\to\mathrm{hadrons}(\gamma)}(s)}{\sigma_{e^+e^-\to\mu^+\mu^-}(s)}, \tag{2.4}$$

where α is the fine-structure constant, and the second equation holds for values of s for which we can neglect the muon mass. The γ in parentheses indicates that hadronic states with final-state radiation are included in addition to purely hadronic states.

In Sec. II A we review the FESRs which relate $R(s)$, which is available from experimental data for $e^+e^- \to$ hadrons, to a theoretical representation of $\Pi(q^2)$ at large q^2. In Secs. II B and II C we review the theoretical representation for large q^2 away from the Minkowski axis $q^2 = s$, based on the OPE. As is well known, the OPE does not capture the nonanalytic behavior of $\Pi(q^2)$ on the positive real q^2 axis that corresponds to the presence of hadronic resonances in $\rho(s)$. In Sec. II D we discuss our method for modeling these "duality-violating" effects and the use of this approach in estimating the systematic uncertainty associated with neglecting duality-violating effects in the determination of α_s from FESR analyses of $\Pi(q^2)$.

A. Finite-energy sum rules

Extending $z = q^2$ to the complex plane, the function $\Pi(z)$ is analytic everywhere except on the positive real z-axis. Therefore, the integral of $\Pi(z)$ times any analytic function of z, along the contour shown in Fig. 1, vanishes. From this, employing Eq. (2.3), one has, for any polynomial weight $w(y)$, the FESR relation

$$\begin{aligned} I^{(w)}(s_0) &\equiv \frac{1}{12\pi^2 s_0}\int_0^{s_0} ds w\left(\frac{s}{s_0}\right)R(s) \\ &= -\frac{1}{2\pi i s_0}\oint_{|z|=s_0} dz w\left(\frac{z}{s_0}\right)\Pi(z). \end{aligned} \tag{2.5}$$

We will use experimental data for $R(s)$ to evaluate the integrals on the left-hand side of Eq. (2.5). As already indicated in Eq. (2.4), these data also include EM corrections, and the threshold value of s is thus equal to m_π^2, corresponding to the opening of the channel $e^+e^- \to \pi^0\gamma$.

[8]We will drop the superscript EM on $\Pi(q^2)$.

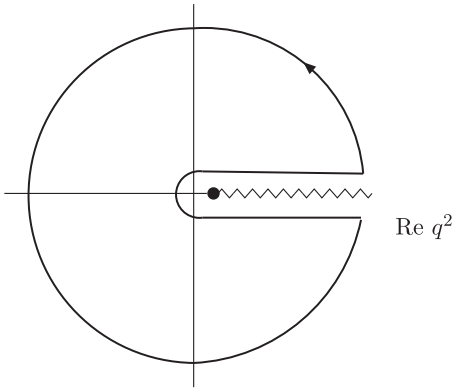

FIG. 1. Analytic structure of $\Pi(q^2)$ in the complex $z = q^2$ plane. There is a cut on the positive real axis starting at $s = q^2 = m_\pi^2$ (see text). The solid curve shows the contour used in Eq. (2.5).

In this paper, we will consider the weights

$$\begin{aligned} w_0(y) &= 1, \\ w_2(y) &= 1 - y^2, \\ w_3(y) &= (1-y)^2(1+2y), \\ w_4(y) &= (1-y^2)^2, \end{aligned} \tag{2.6}$$

where the subscript indicates the degree of the polynomial. The weight $w_2(y)$ has a single zero at $z = s_0$ (a single "pinch"), suppressing contributions from the region near the timelike point $z = s_0$ on the contour. The weights $w_3(y)$ and $w_4(y)$ are doubly pinched, with a double zero at $z = s_0$. All weights are chosen such that no linear term in y appears; the reason for this is discussed in the next section. The weights (2.6) form a linearly independent basis for polynomials up to degree 4 without a linear term.

B. Perturbation theory and the OPE

We begin with splitting $\Pi(z)$ into two parts:

$$\Pi(z) = \Pi_{\mathrm{OPE}}(z) + [\Pi(z) - \Pi_{\mathrm{OPE}}(z)] \equiv \Pi_{\mathrm{OPE}}(z) + \Delta(z), \tag{2.7}$$

where $\Pi_{\mathrm{OPE}}(z)$ is the OPE approximation to $\Pi(z)$,

$$\Pi_{\mathrm{OPE}}(z) = \sum_{k=0}^{\infty}\frac{C_{2k}(z)}{(-z)^k}. \tag{2.8}$$

We will return to $\Delta(z)$ in Sec. II D. Each of the coefficients $C_{2k}(z)$, for $k > 1$, is a sum over contributions from different condensates of dimension $D = 2k$. The $D = 0$ term corresponds to the purely perturbative contribution obtained in massless perturbation theory; the $D = 2$ term to the perturbative contributions proportional to the squares of

the light quark masses. Each contribution depends logarithmically on z, and this dependence can be calculated in perturbation theory. In practice, it is convenient to consider, instead of $\Pi(z)$, the Adler function $D(z) \equiv -z d\Pi(z)/dz$, which is finite and independent of the renormalization scale μ. The $D = 0$ contribution, $D_0(z)$, to $D(z)$ takes the form

$$D_0(z) \equiv -z\frac{dC_0(z)}{dz} = \frac{1}{6\pi^2}\sum_{n=0}^{\infty}\left(\frac{\alpha_s(\mu^2)}{\pi}\right)^n \sum_{k=1}^{n+1} k c_{nk}\left(\log\frac{-z}{\mu^2}\right)^{k-1}, \quad (2.9)$$

where the coefficients c_{nk} are known to five-loop order, i.e., order α_s^4 [2]. It is straightforward to rewrite the $D = 0$ contributions to the right-hand side of Eq. (2.5) in terms of $D_0(z)$ via partial integration. The independence of $D(z)$ on μ implies that only the coefficients c_{n1} are independent; the c_{nk} with $k > 1$ can be expressed in terms of the c_{n1} through use of the renormalization group, resulting in expressions also involving the coefficients of the β function.[9] In the $\overline{\rm MS}$ scheme, $c_{01} = c_{11} = 1$, $c_{21} = 1.63982$, $c_{31} = 6.37101$ and $c_{41} = 49.07570$, for three flavors [2].[10] While c_{51} is not currently known, we will use the estimate $c_{51} = 283$ provided in Ref. [3], to which we assign an uncertainty ± 283. For the running of α_s we use the four-loop $\overline{\rm MS}$ β-function, but we have checked that using five-loop running instead [23] leads to differences of order 10^{-4} or less in our results for α_s at the τ mass.

Beyond the uncertainty in c_{51}, it is common practice to consider different guesses about higher orders in perturbation theory, in order to obtain insight into the effect of neglecting terms beyond those explicitly included in evaluating the $D = 0$ contribution to the right-hand side of Eq. (2.5). Two commonly used prescriptions are fixed-order perturbation theory (FOPT), in which μ is chosen to be a fixed scale, here $\mu^2 = s_0$, and contour-improved perturbation theory (CIPT) [24], in which the scale μ^2 is set equal to $-z$, thus resumming to all orders the running of the coupling point by point along the contour, using the four-loop beta function [so only terms with $k = 1$ survive in Eq. (2.9)]. The two procedures lead to different values of α_s. This difference is a source of systematic uncertainty in this type of analysis.

We next turn to the quadratic, mass-dependent perturbative contributions encoded in the $D = 2$ term, $C_2(z)$, of Eq. (II B). With terms proportional to the squares of the light quark masses $m_{u,d}$ safely negligible, $C_2(z)$ is proportional to m_s^2, the square of the strange quark mass, and takes the form

$$C_2(z) = \frac{m_s^2(\mu^2)}{6\pi^2}\sum_{n=0}^{\infty}\left(\frac{\alpha_s(\mu^2)}{\pi}\right)^n \sum_{k=0}^{n} f_{nk}\left(\log\frac{-z}{\mu^2}\right)^k. \quad (2.10)$$

By choosing $\mu^2 = -z$, one recovers the result derived in Refs. [25], with $f_{00} = 1$, $f_{10} = 8/3$ and $f_{20} = 23.26628$, truncating the series at three-loop order. Here we will use the fixed-order expression with $\mu^2 = s_0$ in Eq. (2.10). The coefficients f_{nk} with $k > 0$ can again be expressed in terms of the f_{n0} by using the renormalization group; they involve the coefficients of the β function and the mass anomalous dimension γ. With the $D = 2$ contribution representing a small correction to the $D = 0$ term,[11] the impact on the values of α_s obtained in our analysis of a shift from the fixed-order to contour-improved scheme for treating the $D = 2$ contribution is safely negligible.[12] We will run the strange quark mass to the scale s_0 from $\mu = m_\tau$, employing the $\overline{\rm MS}$ value $m_s(m_\tau^2) = 97$ MeV as input.[13]

The $D = 4$ term, $C_4(z)$, does not contribute to the sum rules (2.5) if we ignore its logarithmic dependence on z, because none of the weights in Eq. (2.6) contains a term linear in y. The z dependence for these weights enters the right-hand side of Eq. (2.5) only at order α_s^2. These effects were found to be safely negligible in the analogous sum-rule analysis of hadronic τ decay data reported in Ref. [6]. Since in this paper we will work at values of s_0 larger than those employed in the τ-based analysis, it is safe to neglect these effects here as well. This means that the $D = 4$ term plays no role in our analysis. Our avoidance of sum rules involving the $D = 4$ term is motivated by the results of Ref. [28], in which a renormalon-model-based study indicated that perturbation theory for sum rules with such weights is particularly unstable.[14]

We will also ignore the logarithmic z dependence of the higher-order coefficients C_D, with $D \geq 6$, for the simple reason that no complete information on this dependence is available. We note that, of course, the z dependence is again suppressed by a power of α_s. This means that the FESR with weight w_2 will involve C_6, the FESR with weight w_3 will involve C_6 and C_8, and the FESR with weight w_4 will involve C_6 and C_{10}. The presence of C_6 in different sum rules provides an additional consistency check on our fits. As the OPE itself diverges as an expansion in $1/z$, it is safer

[9] See for instance Ref. [21].

[10] In this paper, we will restrict ourselves to the $\overline{\rm MS}$ scheme, even though it may be interesting to investigate other "physical" schemes as well [22].

[11] Its presence shifts the value of α_s by about 1%–2%.

[12] The treatment of the rather similar $D = 2$ OPE series for the flavor $ud - us$ $V + A$ polarization, which is obtained from that in Eq. (2.10) after rescaling by 9 and setting $f_{00} = 1$, $f_{10} = 7/3$, $f_{20} = 19.93$ and $f_{30} = 208.75$, has been studied by comparing lattice and OPE results in Ref. [26]. The results of that study favor the use of three-loop truncation and the FOPT scheme. It is thus reasonable to expect these choices to be optimal here as well.

[13] This corresponds to the 2+1 flavor, $\overline{\rm MS}$ value $m_s(\mu = 2\ {\rm GeV}) = 92$ MeV, taken from Ref. [27].

[14] Earlier considerations along the same lines can be found in Refs. [3,6,21].

to include sum rules with low-degree weights such as w_0 and w_2 in the analysis.

C. EM corrections

Since the experimental data for $R(s)$ include EM corrections, we also have to incorporate such corrections on the right-hand side of the sum rules (2.5). It turns out that the only numerically significant correction is the leading-order correction to the $D = 0$ term [29] and, in our analysis, we thus correct the $n = 0$ term in Eq. (2.9) by the replacement

$$\frac{1}{6\pi^2} c_{01} \to \frac{1}{6\pi^2} c_{01} \left(1 + \frac{\alpha}{4\pi}\right), \tag{2.11}$$

where α is the fine-structure constant. The numerical effect of this replacement is to shift the value for $\alpha_s(m_\tau^2)$ obtained in our analysis by about -0.001. EM corrections subleading to the correction shown in Eq. (2.11) turn out to be completely irrelevant, numerically.

D. Duality violations

We next turn to the contribution of $\Delta(z)$, defined in Eq. (2.7), to the sum rules (2.5). As shown in Refs. [30,31], under the condition that the integral over $w(z/s_0)\Delta(z)$ around the circle with radius s_0 goes to zero for $s_0 \to \infty$, this integral can be rewritten such that the sum rule takes the form

$$\begin{aligned} I^{(w)}(s_0) &= -\frac{1}{2\pi i s_0} \oint_{|z|=s_0} dz w\left(\frac{z}{s_0}\right) \Pi_{\rm OPE}(z) \\ &\quad - \frac{1}{s_0} \int_{s_0}^{\infty} ds w\left(\frac{s}{s_0}\right) \rho_{\rm DV}(s), \\ \rho_{\rm DV}(s) &\equiv \frac{1}{\pi} {\rm Im}\Delta(s). \end{aligned} \tag{2.12}$$

In this form, the origin of the extra term in the FESR becomes clear: the duality-violating part of the spectral function, $\rho_{\rm DV}(s)$, represents the part of the spectral function which is not captured by the OPE. In physical terms, this results from the deviations from the monotonic OPE behavior resulting from the presence of resonances in the spectrum, for large s.

Building on earlier work [32], a framework for the understanding of duality violations in terms of a generalized Borel-Laplace transform of $\Pi(q^2)$ and hyperasymptotics was developed in Ref. [33]. Employing the $1/N_c$ expansion, working in the chiral limit, and assuming that for high energies the spectrum becomes Regge-like in the $N_c \to \infty$ limit, it was shown that, for a given QCD channel, $\rho_{\rm DV}(s)$ can be parametrized as

$$\rho_{\rm DV}(s) = e^{-\delta - \gamma s} \sin(\alpha + \beta s), \tag{2.13}$$

for large s, up to slowly varying logarithmic corrections in the argument of the sine factor, and with $\gamma \sim 1/N_c$ small but nonzero.[15] The parameter β is directly related to the Regge slope, and the parameter γ to the (asymptotic) ratio of the width and the mass of the resonances in a given channel. This form was sufficient for use in the case of hadronic τ decays, where we considered only the nonstrange $I = 1$ channel.[16]

Here, the situation is more complicated. First, the EM current consists of two parts, the $I = 1$ and $I = 0$ parts J_μ^3 and J_μ^8 of Eq. (2.1), respectively. Furthermore, it is not clear whether one can neglect the strange quark mass in the context of duality violations and use the chiral limit result Eq. (2.13) for the strange quark component of the EM current. For $m_s = 0$, $SU(3)$ flavor symmetry implies that the duality-violating parameters δ, γ, β and α in Eq. (2.13) must be the same for the $I = 1$ and $I = 0$ channels. However, the methods of Ref. [33] do not allow for a straightforward generalization to the case of a nonzero quark mass, and this leaves us with the question as to how to parametrize the $I = 0$ part of $\rho_{\rm DV}(s)$.

The $I = 1$ duality-violating contributions to the weighted EM spectral integrals analyzed in this paper can, of course, be estimated using the results of the fits to the $I = 1$ vector channel duality-violation parameters obtained in the analysis of $I = 1$, vector-channel, flavor-ud τ decay data, described in detail in Refs. [6,7,10]. The exponential damping of $\rho_{DV}(s)$ with increasing s means that even a modest increase in s_0 can serve to significantly reduce residual integrated duality-violating contributions. The ability to employ, in the EM case, values of s_0, all of which exceed the maximum possible in τ-decay-based analyses, i.e., $s_0 = m_\tau^2$, is thus a major advantage for the EM study. A useful measure of the potential importance of residual $I = 1$ duality-violating contributions is the ratio of the size of integrated $I = 1$ duality-violating contributions to the corresponding integrated α_s-dependent $D = 0$ OPE contributions (which dominate the explicit α_s dependence of the theory side of the various FESRs). Over the range of s_0 employed in the analysis below, the resulting estimate of this ratio is, e.g., less than 1.2% for the singly pinched weight $w_2(y)$ and less than 0.2% for the doubly pinched weight $w_3(y)$. Such integrated $I = 1$ duality-violating contributions should thus play a negligible role, on the scale of the other errors in the analysis, in determinations of α_s employing these weights.

This, however, still leaves the question of the size of integrated $I = 0$ duality-violating contributions. While $I = 0$ and $I = 1$ duality-violating contributions are in

[15]This form was first used in Ref. [30], and subsequently further studied and employed in Refs. [6,7,10,31,34].

[16]In the case of τ decays we took the parameters in Eq. (2.13) different in the vector and axial channels, reflecting the differences in the resonance locations and widths in the two channels.

principle related by $SU(3)$-flavor symmetry, the breaking of $SU(3)$-flavor shifts the peaks of the duality-violating oscillations in the $I=0$ spectral function associated with excited ϕ states to higher s than duality-violating $I=1$ peaks associated with the corresponding excited ρ resonances. It is thus possible that larger-than-naively-expected integrated $I=0$ duality-violating contributions may be present in the EM analysis.

As a first step to testing this possibility, one may simply consider running the analysis with the range of weights considered here, assuming integrated $I=0$ duality-violating contributions are also negligible. One can check this assumption for self-consistency by comparing the results for α_s and the fitted OPE condensates obtained from differently weighted FESRs, whose dependence on duality-violation parameters is also very different. A lack of agreement in the values obtained from different FESRs would then signal the presence of non-negligible duality violations. As will be described in detail in Sec. IV, within the current precision, this test yields no evidence for the presence of non-negligible duality violations. The results of Ref. [12], however, show that such self-consistency tests can sometimes be passed even in the presence of non-negligible residual duality-violating contributions. In order to be cautious, we have thus also attempted an explicit study of potential $I=0$ duality-violating contributions. Unfortunately, the $R(s)$ data are insufficiently precise to allow an analysis in which independent sets of $I=0$ and $I=1$ duality-violation parameters, in addition to α_s and the relevant set of OPE condensates, are all fit simultaneously. As a result, some simplifying assumptions have to be made.

In order to investigate integrated $I=0$ duality-violating contributions we thus carry out an analysis in which results from the τ-decay-based analysis of Ref. [10] are used as constraints on the $I=1$ EM contributions. This implements, in particular, the constraints on $I=1$ duality-violation parameters known from the τ analysis. The $I=0$ duality-violation parameters are then to be fitted using $R(s)$ data. We stress again that the integrated $I=1$ duality-violating contributions implied by the τ analysis constraints play a very small role in the FESRs that we consider, so this strategy serves simply as a means of investigating whether larger-than-expected integrated $I=0$ duality-violating contributions might be present and affect our final results for α_s. The inclusion of the unpinched weight, $w=1$, in the analysis is particularly useful for this purpose since integrated duality-violating contributions are less suppressed for $w=1$ than for pinched weights, making it more likely that small residual $I=0$ duality-violating contributions can be successfully fitted.

We now provide explicit details of the $I=0$ duality-violation study outlined above. We proceed as follows. First, in considering duality-violation corrections, we will ignore disconnected contributions, which include strange-light mixing, as this is doubly $SU(3)$-flavor and $1/N_c$ suppressed in the EM polarization.[17] Based on the experimental observation that the ρ meson spectrum and the ω meson spectrum are nearly degenerate,[18] we will assume that, far enough above the narrow $\omega(782)$ resonance, the duality-violating part of the nonstrange $I=0$ spectral function is degenerate in shape with that of the $I=1$ spectral function. For the strange $I=0$ part we will use a parametrization as in Eq. (2.13), but not assume that all parameters are the same as those for the nonstrange part. Taking into account the relevant charge factors, we then arrive at the ansatz

$$\rho^{\rm EM}_{\rm duality-violation}(s) = \frac{5}{9} e^{-\delta_1-\gamma_1 s}\sin(\alpha_1+\beta_1 s) + \frac{1}{9} e^{-\delta_0-\gamma_0 s}\sin(\alpha_0+\beta_0 s). \quad (2.14)$$

We emphasize that, while the framework of Ref. [33] provides strong arguments for the use of such an ansatz in the $SU(3)$ chiral limit (in which $\delta_0=\delta_1$, etc.), additional assumptions are needed in order to arrive at this form. The factor $5/9$ has been chosen such that the expression $e^{-\delta_1-\gamma_1 s}\sin(\alpha_1+\beta_1 s)$ corresponds, in the isospin limit, to the duality-violating $I=1$ contribution $\rho^{I=1}_{DV}(s)$ employed in the analysis of hadronic τ decays in Refs. [6,7,10]. The factor $1/9$ is the square of the strange quark charge. In this form, the $I=0$ and $I=1$ duality-violation parameters must become equal in the $SU(3)$ limit. Some shifts are, however, expected away from this limit, e.g., to take into account the fact that the resonance peaks in the strange $I=0$ contributions are shifted to higher s.

Even the form (2.14) is not directly usable given the quality of the data we will be working with, and more simplifications are needed. First, we will take the $I=1$ parameters δ_1, γ_1, α_1 and β_1 and their associated covariances from the sum-rule analysis of hadronic τ-decay data reported in Refs. [7,10]. As we will see below, this strategy is reasonable since $\rho^{I=1}_{\rm DV}(s)$, with parameters taken from the τ analysis, leads to an acceptable description of the $I=1$ component of the R-ratio data. Furthermore, we will take $\beta_0=\beta_1$, as this parameter is directly proportional to the asymptotic Regge slope, which we will assume not to be affected by $SU(3)$ flavor symmetry breaking. Likewise, we

[17]Note that the leading OPE contribution to the sum of disconnected contributions comes from perturbative contributions which are fourth order in the light-quark masses. These contributions to $\rho^{\rm EM}(s)$ are suppressed by a factor of $(m_s^2-m_l^2)^2/(N_c s^2)$, the fourth order mass dependence arising because two mass insertions are required in each of the disconnected loops if the loop integral is to survive after the sum over all of u, d and s running around the loop is performed.

[18]We observe that the first three resonances are nearly degenerate, and have approximately equal width over mass ratios [except the $\omega(782)$, for which the width is restricted by phase space].

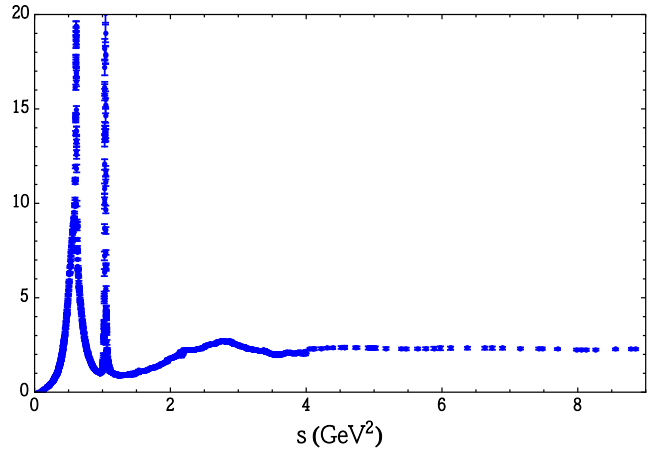

FIG. 2. R-ratio data from Ref. [19], as a function of s, the hadronic invariant squared mass. The three-flavor, massless parton-model value is 2. See Fig. 3 for a comparison with perturbation theory.

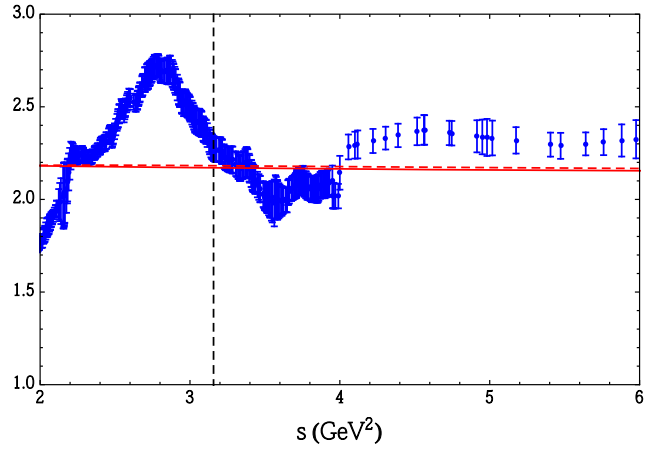

FIG. 3. A blowup of the region $2 \le s \le 6$ GeV^2 in Fig. 2. The red solid and red dashed lines show the results obtained from perturbation theory with $\alpha_s(m_\tau^2) = 0.28$ and $\alpha_s(m_\tau^2) = 0.32$, respectively. The vertical dashed line is $s = m_\tau^2$.

will assume, as an approximation, $\gamma_0 = \gamma_1$,[19] thus leaving us with only the two new free parameters δ_0 and α_0.

All these assumptions put significant limitations on our ability to study duality violations in the case of the EM vacuum polarization. We emphasize however that, as we will see below, our main results for α_s will come from fits for which duality violations can be neglected; fits including duality violations will only serve as a consistency check on our central values and provide us with a means of estimating the systematic uncertainty resulting from neglecting these contributions. In contrast to the case of hadronic τ decays, where data are limited to the region $s \le m_\tau^2$, in the case of $e^+e^- \to$ hadrons we can go to larger s, where duality violations turn out to be less significant, as one would expect.

III. DATA

In this section, we discuss the experimental data for $R(s)$ employed in the fits described in this paper. Our data for $R(s)$ are taken from a new compilation, incorporating all available experimental results, presented first in Ref. [19], where this compilation was used for new determinations of the hadronic vacuum polarization contribution to the muon anomalous magnetic moment and the QED coupling at the scale M_Z, $\alpha(M_Z^2)$.

The data are shown in Fig. 2, where they are plotted against s, the square of the center-of-mass energy for the process $e^+e^- \to$ hadrons(γ). The plot is restricted to results on the interval from $s = 0$ to 9 GeV^2, just below the charm threshold, which, as we will see below, is the region most relevant for our fits. For more figures showing these data, we refer to Ref. [19].

A. Inclusive vs exclusive data

In Fig. 3, we show a blowup of Fig. 2, focusing on the region $2 \le s \le 6$ GeV^2. The vertical axis range shown is centered on the parton-model value, $R = 2$, for this region.

One difference that should be pointed out between the data set used here and that employed in Ref. [19] is the choice concerning the data input for $R(s)$ at about 4 GeV^2. Below this energy, the R-ratio is obtained as a sum over all exclusive hadronic channels. Results for each individual hadronic channel are obtained by combining the available data from many different experiments, where the combination procedure fully incorporates all available correlated uncertainties into the determination of the mean values and uncertainties of the combined cross section. Above about 4 GeV^2, $R(s)$ is instead obtained from the available measured inclusive data (all hadronic channels) using the same procedure to combine the inclusive data from different experiments as with the exclusive channels.[20] The inclusive data combination extends only down to s around 3.39 GeV^2. Moreover, in the lower part of this region, few such data points are available. In principle, one could use

[19]This corresponds to neglecting the difference between the widths of the ρ and ω resonances and the, in general somewhat smaller, widths of the ϕ resonances in the same mass region.

[20]Below about 4 GeV^2, it becomes increasingly difficult to experimentally measure the inclusive R-ratio and requires a detailed understanding of the experimental efficiencies for exclusive states which contribute. Older inclusive measurements do exist slightly below 4 GeV^2 (see the discussions in Refs. [19,35–37] concerning these data). However, these data are imprecise and of poor quality, making them impractical for use in the determination of $R(s)$. In addition, very few of the exclusive states contributing to the hadronic R-ratio have been measured above 4 GeV^2. For details concerning all combined experimental data, we refer to Ref. [19].

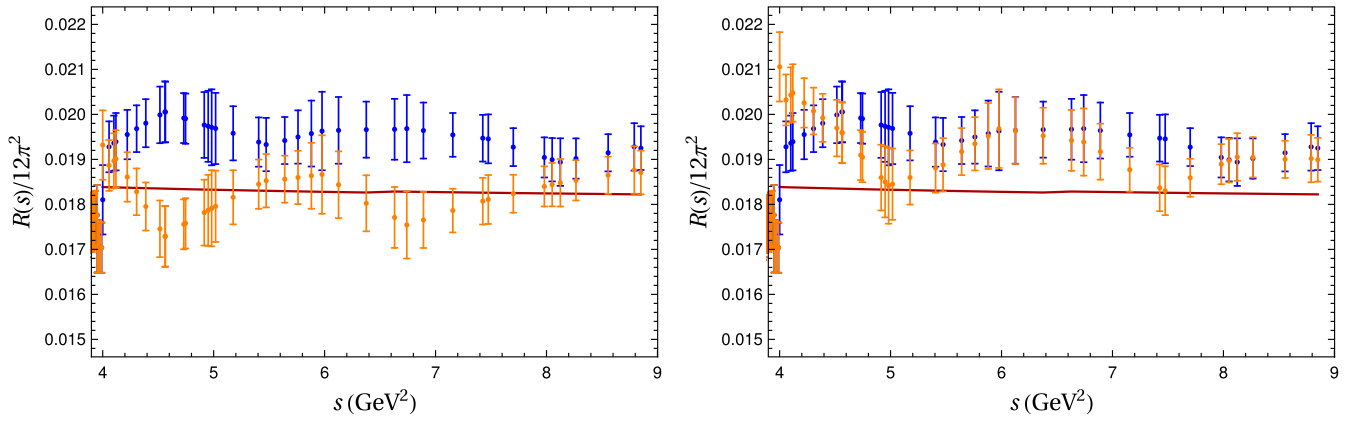

FIG. 4. Two mock data sets generated with the covariance matrix of the real data, in the inclusive region, $4 < s < 9$ GeV^2. The blue data points are the actual data, and the orange data points the mock data. The curve shows perturbation theory with $\alpha_s(m_\tau^2) = 0.3$.

either the sum of exclusive states or the inclusive data combination in the range $3.39 \leq s \leq 4$ GeV^2. In Ref. [19], the choice was made to transition from the sum of exclusive states to the inclusive data at $s \sim 3.75$ GeV^2. However, in the region of overlap, the results obtained by summing exclusive data are more precise. In this work, we have chosen to retain the full information from the sum of exclusive channels up to $s = 4$ GeV^2, for reasons which we will now discuss in more detail.

The determination of α_s from electroproduction in this paper is very similar to that from hadronic τ decays, but has the advantage that the experimental spectral data are kinematically unconstrained and hence are available above $s = m_\tau^2$. We would thus like to use the full range of available R-ratio data, up to at least the charm threshold at $s \sim 9$ GeV^2. However, as we will see below, the errors on the data in the inclusive region, $s > 4$ GeV^2, are too large to allow for a precision determination of α_s in which these data play a major role.

In Fig. 3, we also show the theoretical prediction for $R(s)$ from five-loop perturbation theory (including the six-loop estimate $c_{51} = 283$); the solid red curve corresponds to $\alpha_s(m_\tau^2) = 0.28$, and the dashed red curve to $\alpha_s(m_\tau^2) = 0.32$. The data in the inclusive region $s > 4$ GeV^2 all lie above the perturbative prediction. Contrary to what one might naively conclude, however, this does not imply that the data are inconsistent with the expectations of perturbation theory, but rather reflects the size of the errors and the influence of the strong correlations present in the inclusive data.

In order to investigate this question, we used the actual data covariance matrix to generate several mock data sets drawn from a multivariate Gaussian distribution[21] with central values determined by perturbation theory, i.e., the $D = 0$ part of Eq. (2.8), with $\alpha_s(m_\tau^2) = 0.3$. From a small number of mock data sets we extracted the two sets shown in Fig. 4. The left-hand panel shows a mock data set that, by eye, is perfectly consistent with perturbation theory, while the right-hand panel shows a set very similar to the actual experimental data. These examples demonstrate, visually, that there is no inconsistency between the data and perturbation theory. Instead, the apparent discrepancy between the actual data and perturbation theory is consistent with a statistical fluctuation, one in which the strong correlations in the region play an important role.

One can also investigate the compatibility of the inclusive data with perturbation theory by performing a χ^2 fit of perturbation theory to the $R(s)$ data in the inclusive region. One finds perfectly acceptable fits, with $\chi^2/\text{dof} < 1$, p-values ~ 0.4 and above, corresponding to values of $\alpha_s(m_\tau^2) \sim 0.4 \pm 0.1$ which are within $\sim 1\sigma$ of the current world average but have errors much larger than those achievable in the FESR analysis which is the topic of this paper.

While the outcome of these tests is very reassuring, it also implies that the existing inclusive $R(s)$ data set places only weak constraints on perturbation theory. This is unfortunate, as perturbation theory becomes more reliable at larger s. More precise data would be needed in this region to make an impact on the determination of α_s from electroproduction data. The upshot is that the precision of our electroproduction-based determination of α_s will be almost entirely driven by data from the exclusive region $s \leq 4$ GeV^2.

B. Nature of the peak at $s \sim 2.8$ GeV^2

Next, let us consider the data in the region $2 \leq s \leq 4$ GeV^2. First, even though the determination of α_s benefits primarily from the region $s \leq 4$ GeV^2, we note that this allows us to work at scales significantly higher than the maximum, $s = m_\tau^2 = 3.157$ GeV^2, accessible in hadronic τ decays (shown as the vertical dashed line in Fig. 3). It is, however, clear from Fig. 3 that non-negligible duality violations remain present in the spectral function in this

[21]We note that the experimental covariance matrix is not singular in the region $4 < s < 9$ GeV^2.

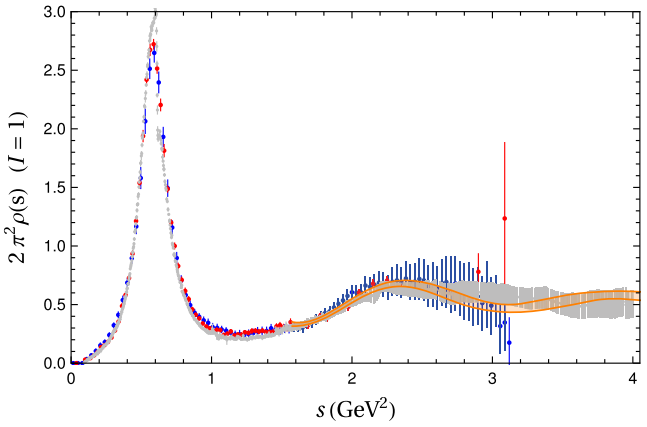

FIG. 5. The $I = 1$ spectral function as a function of s. Shown are the OPAL τ data from Ref. [39] in blue, the ALEPH τ data from Ref. [9] in red, and the $I = 1$ R-ratio data in gray. All data have been normalized such that the parton-model version of the spectral function (not shown in the figure) would be a horizontal line at $2\pi^2\rho(s) = 1/2$. The orange band shows the fit to ALEPH data from Ref. [10] described in Sec. IV B, for s extending down to the lowest value, 1.575 GeV^2, for which the duality-violation ansatz was employed in that fit.

region.[22] The question that remains is, of course, how much they affect the determination of α_s.

To understand this region in more detail, we attempted a separation of the R-ratio data into $I = 0$ and $I = 1$ parts. The result is shown in Fig. 5. This separation follows closely the strategy employed by ALEPH [38] and OPAL [39] in separating vector and axial vector contributions to the nonstrange hadronic τ decay distribution.

In the electroproduction case the separation relies on the observation that the isovector current J^3_μ is G-parity even and the isoscalar current J^8_μ G-parity odd. Up to isospin-breaking corrections, which should be safely small away from the low-s regions near the narrow ω and ϕ resonances, where such corrections can be locally enhanced by resonance interference effects, G-parity can thus be used to uniquely assign the contributions of exclusive modes with well-defined G-parity to either the $I = 0$ or $I = 1$ channel. A significant fraction of the exclusive modes contributing to $R(s)$ in the region below $s = 4$ GeV^2, in fact, have definite G-parity. States consisting of an even (odd) number of pions only, e.g., can be uniquely assigned to the $I = 1$ ($I = 0$) channel. Exclusive states involving, in addition to some number of pions, also a G-parity even η or G-parity odd ω or ϕ are, similarly, uniquely assignable using G-parity. States for which such a unique G-parity assignment is not possible are those containing a $K\bar{K}$ pair not identifiable as coming from the ϕ resonance. Among such states, additional information is available only for $K\bar{K}\pi$, where *BABAR* [40] observed a dominance by K^*K below $s \simeq 4$ GeV^2 and performed a Dalitz plot analysis to separate the $I = 0$ and 1 components of the K^*K cross section. We take advantage of these results. Contributions from modes lacking a unique G-parity assignment, and for which no additional information on the isospin separation is available, are treated in a maximally conservative manner by assigning to each of the $I = 0$ and 1 channels $(50 \pm 50)\%$ of the sum of these contributions. The results of this separation exercise are shown in Fig. 5, for $I = 1$.

This figure shows the data for the $I = 1$ part of the EM spectral function in gray. It shows that these data are in good agreement with data for the corresponding spectral functions obtained from hadronic τ decays by OPAL [39], shown in blue, and ALEPH [9], shown in red. The orange band shows the results of one of the fits of Ref. [10] to the ALEPH τ data, starting from s where the previous analysis suggests the asymptotic duality-violation ansatz (2.13) is valid (described in more detail and employed in Sec. IV B below). To the extent that the τ-based data and the $I = 1$ part of the EM data agree, it is clear that this fit also provides a reasonable representation of the $I = 1$ EM data, although the figure suggests that the $I = 1$ EM data might prefer a somewhat smaller value of β_1 (with accompanying adjustments in the other $I = 1$ parameters).

IV. ANALYSIS

In this section, we will present our main analysis, employing the sum rule (2.5) with weights (2.6). At first, we will ignore duality violations, while retaining all relevant terms in the OPE (2.8), with the assumptions detailed in Sec. II B. To perform these fits, we need the integrated data, as a function of s_0, i.e., the integrals $I^{(w)}(s_0)$ of Eq. (2.5). We perform the fits of these integrals as a function of s_0, ranging from a value $s_0^{\min}$ between 2.5 and 3.8 GeV^2 to $s_0^{\max} = 4$ GeV^2, with the separations of adjacent s_0 as close as possible to $\Delta s_0 = 0.05$ GeV^2. In some cases, it turns out that the integrated data are too strongly correlated to obtain good fits (as measured by their p-value), in which case we enlarge the spacing to $\Delta s_0 \approx 0.1$ GeV^2. We will refer to this procedure as "thinning" by a factor 2. For more details on the use of thinning, we refer to Sec. IV A. It should be noted that even using the spacing $\Delta s_0 \approx 0.05$ GeV^2 corresponds to a thinning of the data, because throughout the spectrum below 4 GeV^2, the binning of the data is much finer than 0.05 GeV^2.

The central values for the weighted spectral integrals $I^{(w_i)}(s_0)$, $i = 0, 2, 3, 4$, on the left-hand side of Eq. (2.5) are obtained from the data using the trapezoidal rule.[23] Despite the fact that the integrated data, i.e., the moments $I^{(w_i)}(s_0)$, are strongly correlated between different values of s_0, we find that these integrated data allow us to perform

[22] Apparent faint oscillations in the inclusive data above 4 GeV^2 are, in contrast, not statistically significant.

[23] We checked that using a different method, such as a histogram rule, makes no significant difference.

TABLE I. Fits to $I^{(w_0)}(s_0)$ from $s_0 = s_0^{\min}$ to $s_0 = s_0^{\max} = 4\,\mathrm{GeV}^2$. FOPT results are shown above the double line, and CIPT below. Fits below the single horizontal lines are used in the average of Eq. (4.1); those marked with an asterisk are thinned by a factor 2.

$s_0^{\min}$ (GeV^2)	Number of dof's	χ^2	p-value	α_s
3.00	20	76.5	2×10^{-8}	0.233(13)
3.15	17	34.6	0.007	0.275(13)
3.25	15	27.8	0.02	0.287(14)
3.00	10*	53.3	7×10^{-8}	0.236(13)
3.15	8*	16.0	0.043	0.279(13)
3.25	7*	9.33	0.23	0.292(14)
3.35	13	19.0	0.12	0.297(14)
3.45	11	14.9	0.19	0.304(14)
3.55	9	14.2	0.12	0.302(15)
3.60	8	10.8	0.21	0.304(15)
3.70	6	7.21	0.30	0.296(16)
3.80	4	6.98	0.14	0.298(17)
3.00	20	76.4	2×10^{-8}	0.236(14)
3.15	17	34.6	0.007	0.282(15)
3.25	15	28.0	0.02	0.295(16)
3.00	10*	53.2	7×10^{-8}	0.239(14)
3.15	8*	16.0	0.04	0.287(16)
3.25	7*	9.64	0.21	0.301(17)
3.35	13	19.6	0.11	0.306(17)
3.45	11	15.7	0.15	0.314(17)
3.55	9	14.9	0.09	0.311(18)
3.60	8	11.6	0.17	0.313(18)
3.70	6	7.65	0.27	0.305(18)
3.80	4	7.46	0.11	0.306(20)

TABLE II. Fits to $I^{(w_2)}(s_0)$ from $s_0 = s_0^{\min}$ to $s_0 = s_0^{\max} = 4\,\mathrm{GeV}^2$. FOPT results are shown above the double line, and CIPT below. Fits below the single horizontal lines are used in the average of Eq. (4.2); those marked with an asterisk are thinned by a factor 2.

$s_0^{\min}$ (GeV^2)	Number of dof's	χ^2	p-value	α_s	C_6 in GeV^6
3.00	19	53.4	0.00004	0.239(13)	−0.0027(13)
3.15	16	25.1	0.07	0.278(14)	0.0033(19)
3.00	9*	38.0	0.00002	0.253(13)	−0.0011(15)
3.15	7*	13.6	0.06	0.287(14)	0.0049(21)
3.25	14	17.3	0.24	0.292(14)	0.0062(23)
3.35	12	13.6	0.33	0.298(15)	0.0078(26)
3.45	10	10.3	0.42	0.305(15)	0.0097(27)
3.50	8	9.45	0.31	0.302(16)	0.0088(30)
3.60	7	9.45	0.22	0.302(16)	0.0088(31)
3.70	5	5.32	0.38	0.293(16)	0.0057(34)
3.80	3	5.14	0.16	0.296(18)	0.0064(38)
3.00	19	53.3	0.00004	0.242(14)	−0.0029(13)
3.15	16	25.2	0.07	0.284(15)	0.0026(17)
3.00	9*	37.9	0.00002	0.257(14)	−0.0013(14)
3.15	7*	13.8	0.06	0.294(16)	0.0040(18)
3.25	14	17.6	0.23	0.298(16)	0.0051(20)
3.35	12	14.0	0.30	0.306(17)	0.0065(22)
3.45	10	10.8	0.37	0.313(17)	0.0081(23)
3.55	8	9.90	0.32	0.309(18)	0.0073(25)
3.60	7	9.90	0.19	0.309(18)	0.0073(26)
3.70	5	5.57	0.35	0.300(18)	0.0045(29)
3.80	3	5.42	0.14	0.302(19)	0.0050(32)

fully correlated fits, on the interval $2.5\ \mathrm{GeV}^2 \le s_0 \le 4.0\ \mathrm{GeV}^2$. It is thus the results of these correlated fits that we present in this paper.

A. Fits

In Table I we show the results for fits using the weight $w_0 = 1$, for a range of choices of $s_0^{\min}$. As the weight w_0 is unpinched, the FESR for this weight is the most susceptible to possible non-negligible duality-violating effects. The first column gives the values of $s_0^{\min}$ employed, and the second column the number of degrees of freedom in the fit, i.e., the number of s_0 values between $s_0^{\min}$ and $s_0^{\max}$ minus the number of parameters in the fit. The third column gives the minimum of χ^2 found in the fit, the fourth column the corresponding p-value, and the final column the value of α_s obtained in the fit. Results above (below) the double horizontal line are obtained using FOPT (CIPT).

It is obvious that the fit quality increases strongly with increasing $s_0^{\min}$, as does the value of α_s, with the latter leveling off when the fits become good, and peaking at $s_0^{\min} \approx 3.45\ \mathrm{GeV}^2$, after which it decreases somewhat. We find that, for $s_0^{\min} = 3.25\ \mathrm{GeV}^2$, the quality of the fits improves significantly if we thin out the data by a factor 2 (i.e., use $\Delta s_0 = 0.1\ \mathrm{GeV}^2$), as shown in Table I: the p-values increase, while the fit parameters remain stable. For $s_0^{\min} < 3.25\ \mathrm{GeV}^2$, there is no clear improvement from thinning out, and p-values are bad or marginal. (We will return to fits with these values of $s_0^{\min}$ in Sec. IV B below.) For higher values of $s_0^{\min}$, the fits are already good and do not improve significantly with thinning. By p-values, the fits with $s_0^{\min}$ ranging from 3.25 to 3.80 GeV^2 are preferred; in the table, they are the fits below the single horizontal lines. Averaging these values of α_s yields the estimates

$$\alpha_s(m_\tau^2)|_{w_0} = \begin{cases} 0.299(15)(6) & \text{(FOPT)}, \\ 0.308(18)(6) & \text{(CIPT)}. \end{cases} \tag{4.1}$$

These values were obtained by a simple average; while one can devise various weighted averages, they all yield very similar results. The first error is the average fit error, the second half the difference between the lowest and highest value entering the average. As Table I shows, the variation in the values of α_s as a function of $s_0^{\min}$ is in fact smaller than the average fit error of ± 0.015 and ± 0.018, for FOPT and CIPT, respectively, and might also be statistical in nature. However, since these values of α_s are highly correlated, it is likely that there is a systematic component as well. Hence, we choose to be conservative, and show the second error as a separate error.

Before we discuss further the results of the fits shown in Table I, we present the results from fits employing the other

TABLE III. Fits to $I^{(w_3)}(s_0)$ from $s_0 = s_0^{\min}$ to $s_0 = s_0^{\max} = 4$ GeV^2. FOPT results are shown above the double line, and CIPT below. Fits below the single horizontal lines are used in the average of Eq. (4.3); those marked with an asterisk are thinned by a factor 2.

$s_0^{\min}$ (GeV^2)	Number of dof's	χ^2	p-value	α_s	C_6 in GeV^6	C_8 in GeV^8
3.15	15	44.8	0.00008	0.276(15)	0.0027(20)	−0.0184(51)
3.25	13	31.9	0.003	0.292(15)	0.0059(23)	−0.0278(61)
3.35	11	26.0	0.006	0.296(15)	0.0068(25)	−0.0305(67)
3.15	6*	9.79	0.13	0.293(15)	0.0055(22)	−0.0261(57)
3.25	5*	7.60	0.18	0.299(15)	0.0070(25)	−0.0307(65)
3.35	4*	5.62	0.23	0.305(16)	0.0084(27)	−0.0353(73)
3.45	9	12.9	0.17	0.303(16)	0.0085(27)	−0.0360(75)
3.55	7	11.6	0.11	0.301(16)	0.0081(29)	−0.0346(83)
3.60	6	11.1	0.09	0.298(17)	0.0071(32)	−0.0311(95)
3.70	4	5.68	0.22	0.292(18)	0.0049(35)	−0.023(11)
3.80	2	2.31	0.32	0.289(19)	0.0036(39)	−0.019(12)
3.15	15	44.9	0.00008	0.279(13)	0.0022(15)	−0.0177(41)
3.25	13	32.2	0.002	0.297(16)	0.0051(20)	−0.0266(56)
3.35	11	26.4	0.006	0.301(17)	0.0059(22)	−0.0290(64)
3.15	6*	9.94	0.13	0.298(16)	0.0047(19)	−0.0250(54)
3.25	5*	7.86	0.16	0.305(17)	0.0061(22)	−0.0293(62)
3.35	4*	5.97	0.20	0.310(17)	0.0074(24)	−0.0336(70)
3.45	9	13.3	0.15	0.308(17)	0.0075(24)	−0.0342(72)
3.55	7	12.0	0.10	0.306(18)	0.0070(26)	−0.0329(79)
3.60	6	11.4	0.08	0.303(18)	0.0061(29)	−0.0294(91)
3.70	4	5.87	0.21	0.297(19)	0.0040(31)	−0.022(10)
3.80	2	2.45	0.29	0.293(20)	0.0028(35)	−0.017(12)

three weights, $w_{2,3,4}$ of Eq. (2.6). They are collected in Tables II to IV. Table II shows good p-values for $s_0^{\min}$ between 3.25 and 3.80 GeV^2; thinning does not appear to improve the fit for $s_0^{\min} = 3.15$ GeV^2. Taking the average of the fits with $s_0^{\min}$ between 3.25 and 3.80 GeV^2 yields

$$\alpha_s(m_\tau^2)|_{w_2} = \begin{cases} 0.298(16)(6) & \text{(FOPT)}, \\ 0.305(18)(7) & \text{(CIPT)}. \end{cases} \tag{4.2}$$

For fits with the weights w_3 and w_4 we find that, for lower values of $s_0^{\min}$, the quality of the fits improves significantly if we thin out the data by a factor 2 (i.e., use $\Delta s_0 = 0.1$ GeV^2), as shown in Tables III and IV: the p-values increase, while, at least for $s_0^{\min} = 3.25$ and 3.35 GeV^2, the fit parameters remain stable. Also the fit with $s_0^{\min} = 3.15$ GeV^2 has a good p-value after thinning, but parameter values are not stable; cf. Table III.[24] For higher values of $s_0^{\min}$, the fits are already good and do not improve significantly with thinning.

Table III shows good p-values for $s_0^{\min}$ between 3.25 and 3.80 GeV^2 if for $s_0^{\min} = 3.25$ and 3.35 GeV^2 we take the thinned fits; taking the average yields

$$\alpha_s(m_\tau^2)|_{w_3} = \begin{cases} 0.298(16)(8) & \text{(FOPT)}, \\ 0.303(18)(8) & \text{(CIPT)}. \end{cases} \tag{4.3}$$

We note that the weight for which we report results in Table IV just trades C_8 for C_{10}, and thus does not increase the number of parameters in the fits. It shows good p-values for $s_0^{\min}$ between 3.45 and 3.80 GeV^2 and for $s_0^{\min} = 3.25$ and 3.35 GeV^2 if we thin as for w_3; taking the average yields

$$\alpha_s(m_\tau^2)|_{w_4} = \begin{cases} 0.297(16)(8) & \text{(FOPT)}, \\ 0.303(18)(8) & \text{(CIPT)}. \end{cases} \tag{4.4}$$

In Fig. 6 we show the fits for the lowest $s_0^{\min}$ value used in the averages reported in Eqs. (4.1)–(4.4). Other fits show equally good visual matches between data and fit curves. The oscillatory behavior as a function of s_0 seen in the data in the upper left panel of Fig. 6 is what one typically expects to see when integrated duality violations are not entirely negligible. Such residual duality violations are expected to be most visible for the unpinched weight w_0. The absence of oscillatory behavior in the other panels is consistent with the suppression of duality violations by the pinching of the other weights.

[24] Fits thinned by a factor 3 (i.e., using $\Delta s_0 = 0.15$ GeV^2) with $s_0^{\min} = 3.15$ GeV^2 cause the p-values to decrease to about 0.05, but yield stable fit parameters in comparison with the fit with $\Delta s_0 = 0.1$ GeV^2. One could, thus, also consider including the results of the thinned fits with $s_0^{\min} = 3.15$ GeV^2 in the average. Since this turns out not to alter the average reported in Eq. (4.3) at the level of accuracy reported there, we choose to average here over the same set of $s_0^{\min}$ used in arriving at the w_2 average in Eq. (4.2). The same comments apply to the w_4 average reported in Eq. (4.4).

TABLE IV. Fits to $I^{(w_4)}(s_0)$ from $s_0 = s_0^{\min}$ to $s_0 = s_0^{\max} = 4$ GeV^2. FOPT results are shown above the double line, and CIPT below. Fits below the single horizontal lines are used in the average of Eq. (4.4); those marked with an asterisk are thinned by a factor 2.

$s_0^{\min}$ (GeV^2)	Number of dof's	χ^2	p-value	α_s	C_6 in GeV^6	C_{10} in GeV^{10}
3.15	15	45.0	0.00008	0.275(15)	0.0027(20)	0.079(14)
3.25	13	32.0	0.002	0.292(15)	0.0060(24)	0.107(17)
3.35	11	26.0	0.006	0.296(15)	0.0069(25)	0.115(19)
3.15	6*	9.76	0.14	0.292(15)	0.0056(22)	0.101(16)
3.25	5*	7.55	0.18	0.299(15)	0.0071(25)	0.115(18)
3.35	4*	5.59	0.23	0.304(15)	0.0086(27)	0.130(21)
3.45	9	12.9	0.17	0.302(16)	0.0087(28)	0.133(22)
3.55	7	11.6	0.11	0.300(16)	0.0082(30)	0.129(25)
3.60	6	11.0	0.09	0.297(17)	0.0072(32)	0.117(30)
3.70	4	5.69	0.22	0.292(18)	0.0050(35)	0.089(34)
3.80	2	2.30	0.32	0.288(19)	0.0037(39)	0.072(40)
3.15	15	45.2	0.00007	0.279(16)	0.0022(17)	0.077(123)
3.25	13	32.3	0.002	0.297(13)	0.0051(15)	0.104(12)
3.35	11	26.4	0.006	0.301(17)	0.0059(22)	0.112(18)
3.15	6*	9.92	0.13	0.298(16)	0.0047(19)	0.098(15)
3.25	5*	7.82	0.17	0.305(17)	0.0061(22)	0.112(18)
3.35	4*	5.96	0.20	0.310(17)	0.0074(24)	0.126(20)
3.45	9	13.3	0.15	0.308(17)	0.0075(24)	0.129(21)
3.55	7	12.0	0.10	0.306(18)	0.0071(26)	0.124(24)
3.60	6	11.4	0.08	0.303(18)	0.0061(29)	0.112(29)
3.70	4	5.90	0.21	0.297(19)	0.0040(31)	0.084(33)
3.80	2	2.44	0.30	0.293(20)	0.0028(35)	0.067(39)

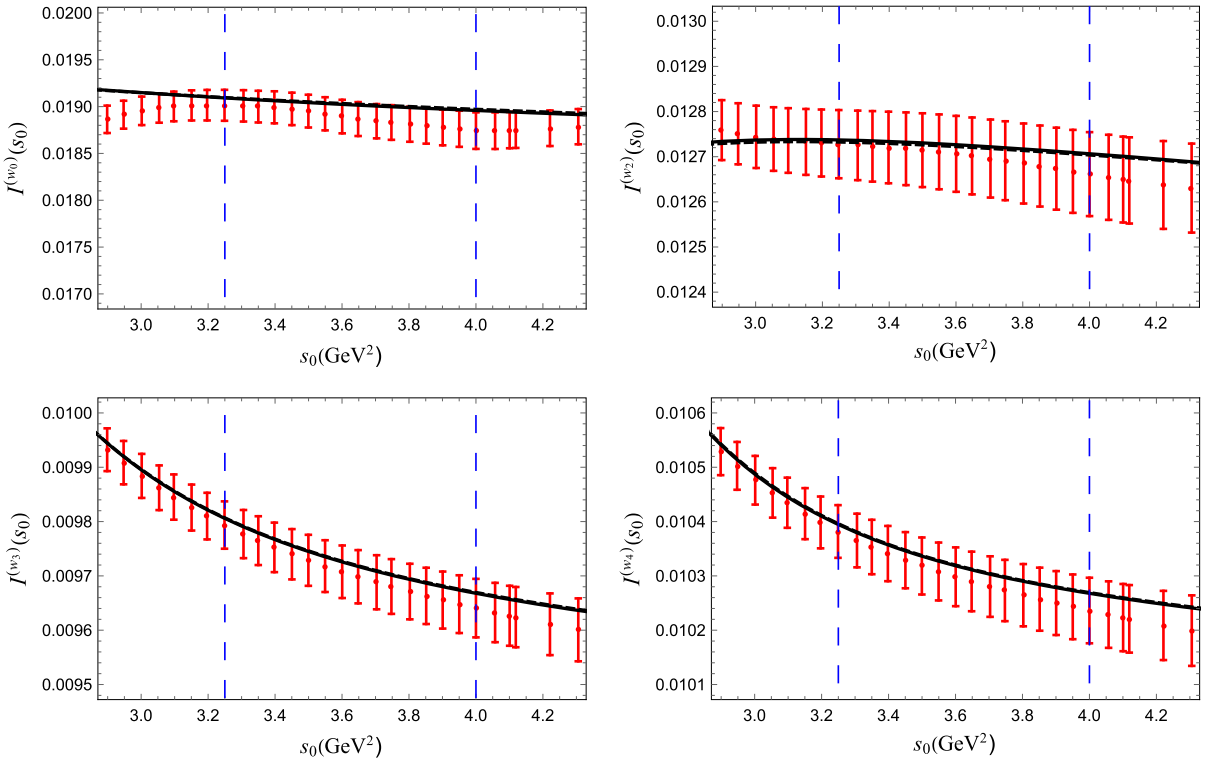

FIG. 6. Comparison of the data for $I^{(w_i)}(s_0)$ with the fits on the interval $s_0^{\min} = 3.25$ to 4 GeV^2, for $i = 0$ (upper left panel), $i = 2$ (upper right panel), $i = 3$ (lower left panel), and $i = 4$ (lower right panel). Solid black curves indicate FOPT fits, dashed curves CIPT. The fit window is indicated by the dashed vertical lines. For $I^{(w_0)}(s_0)$, $I^{(w_3)}(s_0)$ and $I^{(w_4)}(s_0)$ the fit curve is from the thinned fits in Tables I, III and IV, while the data for s_0 values spaced by 0.05 GeV^2 are shown.

The fit qualities (p-values) improve going from weight w_0 to weight w_2, especially for lower values of $s_0^{\min}$, as can be seen by comparing corresponding fits in Tables I and II. This provides additional evidence that pinching indeed suppresses duality violations [whether they are asymptotic, in the sense of being described by Eq. (2.14), or not]. However, this improvement does not appear to persist with more pinching, as can be seen in Tables III and IV. There are several possible reasons for this.

One of these is that the theoretical model underlying the fits with weights w_3 and w_4 may be less good than the one underlying the fit with weight w_2. The higher-degree weights employed in these fits probe higher orders in the OPE, and it is possible that with these higher-D terms we enter the region (at these values of s_0) where the OPE converges less well. An indication of this is that, for s_0 values in the range 3 to 4 GeV^2, the $D = 8$ and $D = 10$ terms are of about the same size as the $D = 6$ term, if we employ the values for $C_{6,8,10}$ reported in these tables, in the $s_0^{\min}$ range with good p-values.[25] A possible interpretation is that use of the weight w_2 provides an optimal balance between suppression of duality violations (because of its zero at $s = s_0$), and the convergence properties of the OPE, in this range. We note that the $D = 6$ contribution is always very small compared to the $D = 0$ (i.e., purely perturbative) term.

Another possibility is statistical in nature. The order of magnitude of the smallest eigenvalues of the correlation matrices for the unthinned fits is 10^{-6} for w_0, 10^{-9} for w_2 and 10^{-12} for w_3 and w_4.[26] The smallness of these eigenvalues, which reflects the very strong correlations between data at different values of s_0, originates in the fact that we integrate the same data to obtain all of the $I^{(w_i)}(s_0)$. While we take the consistency of our results across the different weights (note, in particular, the consistency for both α_s and C_6) as a confirmation of the reliability of the correlated fits, it is possible that the very small eigenvalues in the case of weights w_3 and w_4 result in somewhat larger values of χ^2 for these fits, thus reducing associated p-values. Indeed, we find that the fits with weights w_3 and w_4, for which these lowest eigenvalues are very small, improve by thinning out the data: p-values increase, while fit parameter values remain stable, for $s_0^{\min} = 3.15$, 3.25 and 3.35 GeV^2, as shown in Tables III and IV. Thinning by a factor 2 changes the lowest eigenvalues for these weights from $\sim 10^{-12}$ to $\sim 10^{-9}$. A similar effect occurs for $s_0^{\min} = 3.25$ GeV^2 and weight w_0, where the lowest eigenvalue changes to $\sim 10^{-4}$. For values of $s_0^{\min}$ below 3.25 GeV^2, we typically find no such clear improvement and stability, suggesting a breakdown of the theoretical representation employed in the fits. Indeed, already at $s_0^{\min} = 3.15$ GeV^2 some instability of the fit parameters for weights w_3 and w_4 is visible, even if p-values do improve. For the weight w_2, the p-value does not increase with thinning, for $s_0^{\min} = 3.15$ GeV^2.

Based on the tables, we make the following further observations:

(i) Fits for all weights with $s_0^{\min}$ values lower than those shown in the tables have extremely small p-values, and these fits do not improve with thinning out the data. We attribute this behavior to the fact that, for such s_0, one is in the region where sizable duality violations are present in the spectrum, as evidenced by the peak in $R(s)$ around $s = 2.8$ GeV^2; cf. Figs. 2 and 3. We will return to this point in Sec. IV B.

(ii) All FOPT fits at a given $s_0^{\min}$ are consistent with each other across all these tables, as are all CIPT fits at a given $s_0^{\min}$. Note that not only the values of α_s, but also the values of C_6 are consistent, with C_6 being determined by all fits with pinched weights.

(iii) The difference between FOPT and CIPT results for $\alpha_s(m_\tau^2)$ is about 0.009 from Eq. (4.1), about 0.007 from Eq. (4.2), about 0.005 from Eq. (4.3) and about 0.006 from Eq. (4.4). This is much smaller than corresponding differences obtained from hadronic τ-decay analysis, which are 0.022 from the OPAL data [7] and 0.016 from the ALEPH data [10] (cf. Sec. IV D). The FOPT-CIPT difference is still significant, because, for a given weight and a given $s_0^{\min}$, the FOPT and CIPT values of α_s are very close to 100% correlated.

(iv) The effect of the $D = 2$ term (2.10) is small, but not completely negligible. Its presence has an effect of shifting the values of $\alpha_s(m_\tau^2)$ obtained in our fits by an order of 1%–2%. This confirms that the details of its treatment are indeed insignificant.

B. Tests

Before we use the results thus far obtained to extract a final value for α_s, we perform a number of tests probing the stability of the values reported in Eqs. (4.1)–(4.4). The most important of these is a test for the effects of including the model for duality violations, described in Sec. II D, in the fits.

We have performed fits including Eq. (2.14), as described in Sec. II D. As input we used the results and covariances for α_s and $I = 1$ parameters δ_1, γ_1, α_1 and β_1 from the $s_0^{\min} = 1.575$ GeV^2, vector-channel fit with

[25] It is also worth noting that, from the results in Table IV, the central C_{10} value is large, and it lies many σ's from zero. Using the effective condensates from Tables III and IV, it is also easily shown that the assumption made in a number of τ-based analyses that integrated $D = 10$ and higher contributions can be neglected, relative to integrated lower dimension nonperturbative contributions, for s_0 as large as m_τ^2 would fail quite badly for the analogous EM case considered here.

[26] The smallest eigenvalue in each case is not very sensitive to $s_0^{\min}$, at least in the range $s_0^{\min} = 3.00$ to 3.55 GeV^2. The largest eigenvalue is always of order 10.

TABLE V. Fits to $I^{(w_0)}(s_0)$ from $s_0 = s_0^{\min}$ to $s_0 = s_0^{\max} = 4$ GeV^2. FOPT results are shown above the double line, and CIPT below. The fits include duality violations with input from the determination of Ref. [10] of the $I = 1$ parameters (and α_s) added as priors.

$s_0^{\min}$ (GeV^2)	Number of dof's	χ^2	p-value	α_s	δ_0	α_0
2.75	24	38.6	0.03	0.285(7)	−0.41(55)	3.90(80)
2.85	22	34.4	0.05	0.285(7)	−0.18(58)	3.15(90)
2.95	20	25.8	0.17	0.286(7)	0.20(57)	2.02(94)
3.00	19	21.7	0.30	0.287(7)	0.46(57)	1.4(1.0)
3.15	16	17.0	0.39	0.292(8)	1.15(60)	1.0(1.0)
3.25	14	16.8	0.27	0.291(8)	1.08(67)	0.9(1.1)
3.35	12	13.2	0.36	0.292(9)	1.23(71)	1.1(1.0)
3.45	10	11.9	0.29	0.295(9)	1.48(70)	1.3(1.1)
3.55	8	11.0	0.20	0.293(9)	1.34(74)	1.0(1.2)
3.60	7	8.04	0.33	0.295(9)	1.43(72)	1.1(1.2)
3.70	5	4.37	0.50	0.292(10)	1.34(73)	0.4(1.3)
3.80	3	3.97	0.26	0.292(10)	1.31(74)	0.4(1.4)
2.75	24	37.8	0.04	0.294(8)	−0.49(56)	3.83(80)
2.85	22	33.8	0.05	0.295(8)	−0.30(59)	3.12(91)
2.95	20	25.5	0.18	0.296(9)	0.05(58)	1.97(96)
3.00	19	21.6	0.25	0.297(9)	0.30(58)	1.3(1.0)
3.15	16	17.4	0.36	0.303(10)	0.94(61)	0.9(1.1)
3.25	14	17.1	0.25	0.302(10)	0.85(69)	0.8(1.1)
3.35	12	13.6	0.33	0.303(11)	0.98(72)	0.9(1.1)
3.45	10	12.4	0.26	0.306(11)	1.22(73)	1.2(1.1)
3.55	8	11.5	0.11	0.304(12)	1.08(76)	0.8(1.2)
3.60	7	8.56	0.29	0.306(12)	1.18(75)	1.0(1.2)
3.70	5	4.84	0.44	0.302(12)	1.09(76)	0.2(1.3)
3.80	3	4.43	0.22	0.302(12)	1.06(77)	0.2(1.5)

weight w_0 to the ALEPH data for the nonstrange vector-channel spectral function obtained from hadronic τ decays [9], reported in Ref. [10]; the FOPT fit version of the $I = 1$ spectral function predicted by this fit is graphically shown as the orange band in Fig. 5. The fit was performed by adding a prior to our χ^2 function, employing the full, five-parameter covariance matrix obtained in these fits. Explicitly, we add to the χ^2 function from the $R(s)$ data the term

$$\chi^2_\tau(\boldsymbol{p}) = (\boldsymbol{p} - \bar{\boldsymbol{p}}_\tau) \cdot (C^{(\bar{p}\,\bar{p})})^{-1} \cdot (\boldsymbol{p} - \bar{\boldsymbol{p}}_\tau), \qquad (4.5)$$

where $\boldsymbol{p}$ is the vector of parameters that are being fitted, $\bar{\boldsymbol{p}}_\tau$ are the central values of these parameters from the τ-based fits, and $C^{(\bar{p}\,\bar{p})}$ is the corresponding covariance matrix. We expect such a constrained fit to work because of the excellent consistency between the value of α_s obtained from the τ-based analysis with that obtained here from $R(s)$. The χ^2 value of constrained fit serves as a diagnostic for this: if these values were not consistent, it would result in a bad χ^2 for the constrained fit. The FOPT or CIPT results from Ref. [10] were used, respectively, for our FOPT or CIPT fits of the R-ratio data.

We report the results of fits including Eq. (2.14) in the w_0 sum rule in Table V. In this table, to save space, we do not report the $I = 1$ duality-violating parameters, but note that they are always consistent with the prior parameter values. We do show the values of the $I = 0$ parameters δ_0 and α_0.[27] The errors on $\alpha_s(m_\tau^2)$ are smaller than those reported in Table I; the reason for this is the fact that we added the results of Ref. [10], including the value of α_s, as priors. Since the goal of this study is an $R(s)$-based determination of α_s, the results for α_s reported in Table V are not used in fixing the central values reported in Sec. IV C; they are, instead, used only to estimate the uncertainty induced by the presence of residual duality violations on these central results.[28]

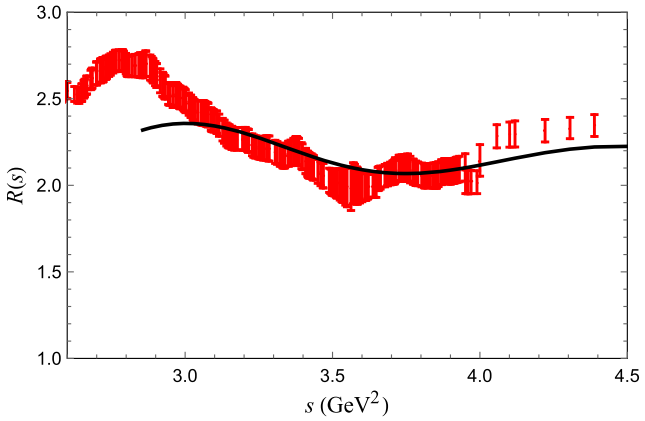

FIG. 7. Spectral representation of the FOPT fit of $I^{(w_0)}(s_0)$ with $s_0^{\min} = 3.15$ GeV^2 of Table V.

From this table, one observes that fits to much lower values of $s_0^{\min}$ now have decent p-values, yielding values for $\alpha_s(m_\tau^2)$ which are significantly more stable as a function of $s_0^{\min}$ than those reported in Table I. However, the decrease of p-values toward lower $s_0^{\min}$, as well as the "wandering" values of δ_0 and α_0, suggest that the ansatz (2.14) may not adequately describe duality violations for values of $s_0 \lesssim 3.0$ GeV^2. We ascribe this to the sizable duality-violating peak around $s = 2.8$ GeV^2 seen in Fig. 3, which is a feature of the $I = 0$ part of the R-ratio data, as it is not seen in the $I = 1$ part shown in Fig. 5. We conclude that for $I = 0$, the asymptotic region in which Eq. (2.14) is conjectured to hold is probably not yet reached for $s \lesssim 3$ GeV^2. We show the spectral function corresponding to the FOPT fit of Table V with $s_0^{\min} = 3.15$ GeV^2 in Fig. 7. This figure confirms that it is very difficult to fit the peak around $s = 2.8$ GeV^2 with the ansatz (2.14), while a reasonable representation is obtained for $s \gtrsim 3$ GeV^2.[29]

[27]Recall that in our model of Sec. II D we set $\gamma_0 = \gamma_1$ and $\beta_0 = \beta_1$.

[28]A combined determination from these data as well as hadronic τ-decay data may be interesting in its own right.

[29]Recall that the apparent mismatch in the inclusive region above 4 GeV^2 is not excluded by the data in that region; cf. Sec. III A.

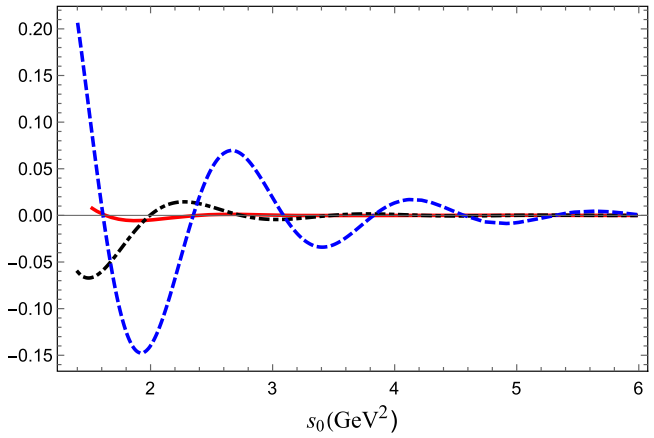

FIG. 8. The contribution from duality violations to the weighted spectral integrals with weights w_0 (blue dashed curve), w_2 (black dotted-dashed curve) and w_3 (red solid curve), as a function of s_0, normalized to the difference between perturbation theory [$D = 0$ term in Eq. (2.8)] and the parton model contribution. The duality-violating parameters employed are those from the FOPT, $s_0^{\min} = 3.15\ \mathrm{GeV}^2$ fit of $I^{(w_0)}(s_0)$ reported in Table V.

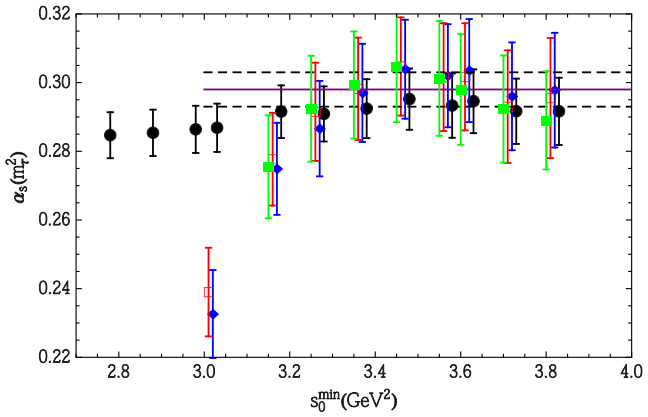

FIG. 9. The FOPT strong coupling $\alpha_s(m_\tau^2)$ as a function of $s_0^{\min}$. Blue data points (diamonds) represent values of $\alpha_s(m_\tau^2)$ from Table I, red (open squares) those from Table II, green (filled squares) those from Table III, and black data points (filled circles) correspond to the values from Table V. The solid, purple horizontal line shows the value 0.298, with the dashed horizontal lines showing the values 0.298 ± 0.005. The red, blue and black data points have been slightly offset horizontally for visibility.

Figure 8 shows the contributions from duality violations to weighted integrals for w_0 (blue dashed curve), w_2 (black dotted-dashed curve) and w_3 (red solid curve), as a function of s_0, normalized to the α_s-dependent part of the integrated perturbative contribution (the difference between the full perturbation theory result and the parton model contribution), employing the duality-violating parameters from the FOPT, $s_0^{\min} = 3.15\ \mathrm{GeV}^2$ fit of Table V. This ratio quantifies the size of integrated duality violations on the scale of the α_s-dependent integrated $D = 0$ contributions from which we aim to determine α_s. This figure illustrates how pinching indeed suppresses duality violations, for those values of s for which the asymptotic behavior of Eq. (2.14) applies. As we have seen, this appears to work reasonably well for $I = 1$ (cf. Fig. 5) for $s \gtrsim 1.6\ \mathrm{GeV}^2$, but may only work for $I = 0$ for $s \gtrsim 3\ \mathrm{GeV}^2$. It is clear that the effect of pinching is significant, and more so in the region above the τ mass ($s = 3.157\ \mathrm{GeV}^2$) than below. We note that this figure should be taken as indicative only, because the data do not allow a full investigation of duality violations in the $I = 0$ channel, for which no information is provided by τ decays.

As can be seen from the dotted-dashed black and solid red curves in Fig. 8, single-weight fits with duality violations and pinched weights $w_{2,3,4}$ are unlikely to effectively constrain duality violations. Nevertheless, we found that fits to $I^{(w_2)}(s_0)$ are possible, with results that are fully compatible with Table V for α_s, δ_0 and α_0. Analogous fits for w_3 and w_4, for which duality violations are even more suppressed, are, unsurprisingly, not stable.

Using now the range $s_0^{\min} \in \{3.15, 3.80\}\ \mathrm{GeV}^2$, we distill the results in Table V into the following estimates for $\alpha_s(m_\tau^2)$. We apply the same procedure as in Sec. IV A and find

$$\alpha_s(m_\tau^2)|_{w_0}^{\mathrm{DV}} = \begin{cases} 0.293(9)(2) & (\mathrm{FOPT}), \\ 0.304(11)(2) & (\mathrm{CIPT}). \end{cases} \tag{4.6}$$

Given the caveats with our investigation of duality violations, we use these results only to estimate the size of the systematic error associated with the presence of duality violations in the region above $s = 3\ \mathrm{GeV}^2$. We see that (a) the value of $\alpha_s(m_\tau^2)$ stabilizes when duality violations are included and (b) that it is lower by 0.006 (0.004), for FOPT (CIPT), from comparing Eq. (4.1) with Eq. (4.6).

As an example of the impact of integrated duality violations on FESRs involving pinched weights, we note that, for w_2 and w_3, the maximum sizes of integrated duality-violating contributions relative to integrated α_s-dependent $D = 0$ terms shown in Fig. 8, in the range of s_0 entering the averages (4.2) and (4.3), are 0.3% and 0.07%, respectively. The maximum shift induced in α_s at a single s_0 in this region is then less than 0.001 in both cases, much smaller than any of the other errors in the analysis.

We will take an error of ± 0.005 as the systematic error from duality violations. This estimate reflects the difference between the results quoted in Eqs. (4.1) and (4.6), and also safely incorporates the variations in the results reported in Eqs. (4.1)–(4.4). We do not also include the second errors shown in Eqs. (4.1)–(4.6), because it is very likely that the spread in values among Eqs. (4.1)–(4.6) is measuring essentially the same uncertainty, insofar as these second errors are due to systematic effects.

The result is illustrated in Fig. 9 for FOPT, which shows values of $\alpha_s(m_\tau^2)$ as a function of $s_0^{\min}$ from Table I (blue diamonds), Table II (red open squares), Table III (green filled squares), and Table V (black filled circles). Also shown is the central value for $\alpha_s(m_\tau^2)$ obtained in Eq. (4.2) (purple

TABLE VI. Fits to $I^{(w_0)}(s_0)$ from varying $s_0 = s_0^{\min}$ to varying $s_0^{\max}$. FOPT results are shown above the double line, and CIPT below. The fits marked with an asterisk are thinned by a factor 2.

$s_0^{\min}$ (GeV^2)	$s_0^{\max}$ (GeV^2)	Number of dof's	χ^2	p-value	α_s
3.25	4.98	14*	22.5	0.07	0.297(13)
3.25	8.85	26*	32.8	0.17	0.299(13)
3.55	8.85	23*	26.8	0.26	0.310(14)
4.10	8.85	18*	16.5	0.56	0.280(21)
6.13	8.85	15	15.6	0.41	0.302(24)
3.25	4.98	14*	21.9	0.08	0.309(16)
3.25	8.85	26*	32.4	0.18	0.310(16)
3.55	8.85	23*	26.9	0.26	0.321(17)
4.10	8.85	18*	16.1	0.59	0.288(24)
6.13	8.85	15	14.8	0.46	0.314(28)

horizontal line), with variations ± 0.005 (dashed horizontal lines). The figure does not show the values reported in Table IV, to avoid clutter. However, these additional fits do not change the picture. For the sake of brevity we do not show the analogous CIPT results as these are very similar.

We investigated several other systematic issues. One of these is the unknown value of the perturbative six-loop Adler coefficient, c_{51}, for which we used an estimate $c_{51} = 283$. Varying the value of this coefficient by ± 283, we find, on average, a variation of about ± 0.003 in the fitted values for $\alpha_s(m_\tau^2)$. We will thus allow for an additional systematic error equal to ± 0.003.

We also considered extending the range of s_0 values over which we fit to values larger than 4 GeV^2. We show examples of such fits of $I^{(w_0)}(s_0)$ in Table VI, for both FOPT and CIPT. The first three fits in each case have $s_0^{\min}$ below 4 GeV^2, in the exclusive data region, and $s_0^{\max}$ larger than 4 GeV^2, in the inclusive data region. The other two have both $s_0^{\min}$ and $s_0^{\max}$ in the inclusive data region. Given the rapid decrease of integrated duality violations with increasing s_0 (see Fig. 8), and the fact that the impact of integrated duality violations on α_s was already seen to be small for the lower s_0 of purely exclusive region fits, we expect such duality-violating contributions to be safely negligible for fits with both $s_0^{\min}$ and $s_0^{\max}$ in the inclusive region, even for w_0. In most cases, indicated in the table, thinning was needed to obtain good fits. We see that extending $s_0^{\max}$ into the inclusive region yields results in good agreement with the results of Sec. IV A used in the averages, with similar errors. While the individual errors are competitive with those in Table I when $s_0^{\min} < 4$ GeV^2, the spread between different fits becomes larger. We should also emphasize the importance of correlations when considering the results of these fits. For example, taking into account correlations, we have verified that the larger differences between the α_s values obtained with $s_0^{\max} = 8.85$ GeV^2 and $s_0^{\min}$ varying from 3.55 GeV^2 to 4.10 GeV^2 are consistent with statistical fluctuations.

Similar results can be obtained for the weights w_2, w_3 and w_4 and are again in good agreement with the results of Sec. IV A, although typically for these weights thinning with a factor larger than 2 is necessary to obtain good fits. We therefore will only use our fits with all data in the exclusive region to obtain our central values, considering the fits of Table VI as a consistency check. In short, the data in the inclusive region appear to be consistent with those below $s = 4$ GeV^2, but with the current precision, they do not improve the accuracy in the value of α_s that can be obtained from R-ratio data. This consistency with the analysis involving only the exclusive data justifies quoting the results with the smallest total errors, which are those of the exclusive-data-only analysis.

C. Results

Following the analysis of Secs. IV A and IV B, we quote as our central results for the strong coupling from the R-ratio data of Ref. [19] the $\overline{\text{MS}}$, three-flavor values

$$\alpha_s(m_\tau^2) = \begin{cases} 0.298 \pm 0.016 \pm 0.005 \pm 0.003 = 0.298 \pm 0.017 & \text{(FOPT)}, \\ 0.304 \pm 0.018 \pm 0.005 \pm 0.003 = 0.304 \pm 0.019 & \text{(CIPT)}. \end{cases} \tag{4.7}$$

The first error is the average fit error, the second error our estimate of the uncertainty produced by residual duality violations, and the third error is due to the variation in c_{51}. Since these errors may be considered as independent, we combine them in quadrature to obtain our final aggregate errors. While we quote values for FOPT and CIPT separately, their difference should be interpreted as another systematic error, representing our incomplete knowledge of higher orders in perturbation theory. While the difference, equal to 0.006, is small, it is nonetheless significant, because the FOPT and CIPT values for $\alpha_s(m_\tau^2)$ are essentially 100% correlated.

These three-flavor results convert to the following five-flavor results at the Z mass:

$$\alpha_s(m_Z^2) = \begin{cases} 0.1158 \pm 0.0022 & (\overline{\text{MS}}, n_f = 5, \text{FOPT}), \\ 0.1166 \pm 0.0025 & (\overline{\text{MS}}, n_f = 5, \text{CIPT}). \end{cases} \tag{4.8}$$

The central values are somewhat low compared to the PDG world average of 0.1181 ± 0.0011 [41] and also compared to the recent high-accuracy value 0.11852 ± 0.00084 of Ref. [42], but are consistent with these results within errors.

D. Comparison with the determination from hadronic τ decays

We can also compare our results with those obtained from the recent analyses of OPAL and ALEPH hadronic τ-decay data reported in Refs. [7,10]. A combination of these results yielded [10]

$$\alpha_s(m_\tau^2) = \begin{cases} 0.303 \pm 0.009 & (\overline{\rm MS}, n_f = 3, {\rm FOPT}), \\ 0.319 \pm 0.012 & (\overline{\rm MS}, n_f = 3, {\rm CIPT}). \end{cases} \quad (4.9)$$

These values are in excellent agreement with Eq. (4.7), differing by 0.3 and, respectively, 0.7σ. While the τ-based values have smaller total errors, we note that the difference between FOPT and CIPT values is larger for the values obtained from τ decays, in comparison with the values we obtained here from electroproduction, making the electroproduction-based determination more competitive with the τ-based determination than the errors shown in Eqs. (4.7) and (4.9) indicate. We also reiterate that duality violations play a significantly larger role in the τ-based analyses, where the sum rules are limited by kinematics to lower values of s_0 [12].[30]

V. CONCLUSION

Recently, a new compilation of the hadronic R-ratio from all available experimental data for the process $e^+e^- \to$ hadrons(γ) became available [19]. In this paper, we used finite-energy sum rules for a determination of the strong coupling based on these data.

In contrast to the case of hadronic τ decays, there is no inherent limit on s in $e^+e^- \to$ hadrons(γ), and this allowed us to go to higher energies, where we need to rely less on models to take into account the nonperturbative effects associated with violations of quark-hadron duality. In a marked difference, only the errors in our determination, Eq. (4.7), required the modeling of duality violations, whereas in the case of τ decays, duality-violating contributions had to be included in all self-consistent fits employed to extract α_s from the data. Because $e^+e^- \to$ hadrons(γ) allowed us to probe energies above the τ mass, and because of the exponential, and hence fairly rapid, decay of the strength of duality violations, we were able to obtain stable results for α_s from sum rules which on the theory side involve only the OPE. This was not *a priori* obvious, considering that the inclusion of the effects from duality violations has been shown to be important for the determination of α_s from τ decays [12]. It is thus a nontrivial result that the values for α_s that we obtain from the R-ratio are in very good agreement with the values for α_s obtained from τ decays. They are also consistent within errors, when converted to values at the Z mass, with the world average as reported in Ref. [41], albeit with somewhat lower central values. This result provides a nontrivial test, at the current level of precision, of the perturbative running of α_s predicted by QCD even at rather low scales, a result which is far from obvious [43].

As has become common in these determinations from finite-energy sum rules, we reported two values for α_s, corresponding to two different assumptions about how to resum unknown higher orders in perturbation theory, FOPT and CIPT. The difference represents our ignorance of these higher orders, assuming that, at these energies, we have not yet reached the order in perturbation theory where its asymptotic nature becomes manifest [3]. The difference between CIPT and FOPT that we find from the R-ratio is smaller than the one found in hadronic τ decays. It is likely that some of this reduction can be ascribed to the extraction of α_s using sum rules at a higher s_0. However, since the convergence properties of the perturbative expansions for the various (linear combinations of) moments of the spectral function are not universal [28], it is not clear that a direct comparison of this difference between the determinations from the R-ratio and τ decays can be made. It is for this reason that we refrain from just adding the difference between FOPT and CIPT as another systematic error to the total error in our determinations of α_s.

Our final result, Eq. (4.7), shows that the largest error is the fit error, which is experimental in nature. This implies that more precise future data for the R-ratio would help in making the determination from the R-ratio more precise and provide a more stringent test on the workings of QCD perturbation theory at lower energies. The biggest impact on our determination comes from the region below 2 GeV, where the R-ratio is compiled from very many carefully measured exclusive-channel contributions. While much improved inclusive data in the region between 2 and 3 GeV have more recently become available [16–18], we found that, at present, these inclusive data do not have much impact on the precision of our determination. In this respect, prospects for the release of new inclusive R-ratio data by BESIII [44] and the experiments at Novosibirsk (SND, CMD-3, KEDR) are potentially promising. In addition, efforts at Novosibirsk to determine the inclusive R-ratio at lower energies than 2 GeV [45] would allow further study into the choices of the transition region between the sum of exclusive states and the inclusive data.

In the meantime, a project that may be worth considering is a determination of α_s combining hadronic R-ratio data and τ-decay data. Such an approach appears to be sensible in view of the consistency between our determinations of α_s from each of these separately.

ACKNOWLEDGMENTS

We like to thank Claude Bernard and Matthias Jamin for helpful discussions. D. B., A. K. and K. M. would like to thank the Institut de Física d'Altes Energies (IFAE) at the Universitat Autònoma de Barcelona for hospitality.

[30] This has been disputed in Ref. [11].

The work of D. B. is supported by the São Paulo Research Foundation (Fundação de Amparo `a Pesquisa do Estado de São Paulo) Grant No. 2015/20689-9 and by Conselho Nacional de Desenvolvimento Científico e Tecnológico (CNPq) Grant No. 305431/2015-3. The work of M. G. is supported by the U.S. Department of Energy, Office of Science, Office of High Energy Physics, under Award No. DE-FG03-92ER40711. The work of A. K. is supported by Science and Technology Facilities Council (STFC) under the Consolidated Grant No. ST/N504130/1. K. M. is supported by a grant from the Natural Sciences and Engineering Research Council of Canada. The work of D. N. is supported by Japan Society for the Promotion of Science (JSPS KAKENHI) Grants No. JP16K05323 and No. JP17H01133. S. P. is supported by Comisión Interministerial de Ciencia y Tecnología Fondo Europeo de Desarrollo Regional (CICYTFEDER) CICYTFEDER-FPA2014-55613-P, 2014-SGR-1450. The work of T. T. is supported by STFC under the Consolidated Grant No. ST/P000290/1.

[1] G. P. Salam, arXiv:1712.05165.
[2] P. A. Baikov, K. G. Chetyrkin, and J. H. Kühn, Phys. Rev. Lett. **101**, 012002 (2008).
[3] M. Beneke and M. Jamin, J. High Energy Phys. 09 (2008) 044.
[4] K. Maltman and T. Yavin, Phys. Rev. D **78**, 094020 (2008).
[5] I. Caprini and J. Fischer, Eur. Phys. J. C **64**, 35 (2009).
[6] D. Boito, O. Catà, M. Golterman, M. Jamin, K. Maltman, J. Osborne, and S. Peris, Phys. Rev. D **84**, 113006 (2011).
[7] D. Boito, M. Golterman, M. Jamin, A. Mahdavi, K. Maltman, J. Osborne, and S. Peris, Phys. Rev. D **85**, 093015 (2012).
[8] G. Abbas, B. Ananthanarayan, I. Caprini, and J. Fischer, Phys. Rev. D **87**, 014008 (2013); I. Caprini, Mod. Phys. Lett. A **28**, 1360003 (2013); G. Abbas, B. Ananthanarayan, and I. Caprini, Mod. Phys. Lett. A **28**, 1360004 (2013).
[9] M. Davier, A. Hoecker, B. Malaescu, C. Z. Yuan, and Z. Zhang, Eur. Phys. J. C **74**, 2803 (2014).
[10] D. Boito, M. Golterman, K. Maltman, J. Osborne, and S. Peris, Phys. Rev. D **91**, 034003 (2015).
[11] A. Pich and A. Rodríguez-Sánchez, Phys. Rev. D **94**, 034027 (2016).
[12] D. Boito, M. Golterman, K. Maltman, and S. Peris, Phys. Rev. D **95**, 034024 (2017).
[13] R. Shankar, Phys. Rev. D **15**, 755 (1977); R. G. Moorhouse, M. R. Pennington, and G. G. Ross, Nucl. Phys. **B124**, 285 (1977); K. G. Chetyrkin and N. V. Krasnikov, Nucl. Phys. **B119**, 174 (1977); K. G. Chetyrkin, N. V. Krasnikov, and A. N. Tavkhelidze, Phys. Lett. **76B**, 83 (1978); N. V. Krasnikov, A. A. Pivovarov, and N. N. Tavkhelidze, Z. Phys. C **19**, 301 (1983); E. G. Floratos, S. Narison, and E. de Rafael, Nucl. Phys. **B155**, 115 (1979); R. A. Bertlmann, G. Launer, and E. de Rafael, Nucl. Phys. **B250**, 61 (1985).
[14] E. Braaten, Phys. Rev. Lett. **60**, 1606 (1988).
[15] E. Braaten, S. Narison, and A. Pich, Nucl. Phys. **B373**, 581 (1992).
[16] J. Z. Bai *et al.* (BES Collaboration), Phys. Rev. Lett. **84**, 594 (2000); **88**, 101802 (2002).
[17] M. Ablikim *et al.* (BES Collaboration), Phys. Lett. B **677**, 239 (2009).
[18] V. V. Anashin *et al.*, Phys. Lett. B **753**, 533 (2016); **770**, 174 (2017).
[19] A. Keshavarzi, D. Nomura, and T. Teubner, Phys. Rev. D **97**, 114025 (2018).
[20] M. Davier, A. Hoecker, B. Malaescu, and Z. Zhang, Eur. Phys. J. C **77**, 827 (2017).
[21] M. Jamin, J. High Energy Phys. 09 (2005) 058.
[22] D. Boito, M. Jamin, and R. Miravitllas, Phys. Rev. Lett. **117**, 152001 (2016).
[23] P. A. Baikov, K. G. Chetyrkin, and J. H. Kühn, Phys. Rev. Lett. **118**, 082002 (2017); F. Herzog, B. Ruijl, T. Ueda, J. A. M. Vermaseren, and A. Vogt, J. High Energy Phys. 02 (2017) 090.
[24] A. A. Pivovarov, Z. Phys. C **53**, 461 (1992); Yad. Fiz. **54**, 1114 (1991) [Sov. J. Nucl. Phys. **54**, 676 (1991)]; F. Le Diberder and A. Pich, Phys. Lett. B **286**, 147 (1992).
[25] S. G. Gorishnii, A. L. Kataev, and S. A. Larin, Nuovo Cimento Soc. Ital. Fis. **92A**, 119 (1986); K. G. Chetyrkin and J. H. Kühn, Phys. Lett. B **248**, 359 (1990).
[26] R. J. Hudspith, R. Lewis, K. Maltman, and J. Zanotti, Phys. Lett. B **781**, 206 (2018).
[27] S. Aoki *et al.*, Eur. Phys. J. C **77**, 112 (2017).
[28] M. Beneke, D. Boito, and M. Jamin, J. High Energy Phys. 01 (2013) 125.
[29] A. L. Kataev, Phys. Lett. B **287**, 209 (1992); L. R. Surguladze, arXiv:hep-ph/9803211.
[30] O. Catà, M. Golterman, and S. Peris, J. High Energy Phys. 08 (2005) 076.
[31] O. Catà, M. Golterman, and S. Peris, Phys. Rev. D **77**, 093006 (2008).
[32] B. Blok, M. A. Shifman, and D. X. Zhang, Phys. Rev. D **57**, 2691 (1998); **59**, 019901(E) (1998); I. I. Y. Bigi, M. A. Shifman, N. Uraltsev, and A. I. Vainshtein, Phys. Rev. D **59**, 054011 (1999); M. A. Shifman, arXiv:hep-ph/0009131; M. Golterman, S. Peris, B. Phily, and E. de Rafael, J. High Energy Phys. 01 (2002) 024.
[33] D. Boito, I. Caprini, M. Golterman, K. Maltman, and S. Peris, Phys. Rev. D **97**, 054007 (2018).
[34] O. Catà, M. Golterman, and S. Peris, Phys. Rev. D **79**, 053002 (2009).
[35] K. Hagiwara, A. D. Martin, D. Nomura, and T. Teubner, Phys. Rev. D **69**, 093003 (2004).
[36] K. Hagiwara, A. D. Martin, D. Nomura, and T. Teubner, Phys. Lett. B **649**, 173 (2007).
[37] K. Hagiwara, R. Liao, A. D. Martin, D. Nomura, and T. Teubner, J. Phys. G **38**, 085003 (2011).

[38] R. Barate *et al.* (ALEPH Collaboration), Eur. Phys. J. C **4**, 409 (1998); S. Schael *et al.* (ALEPH Collaboration), Phys. Rep. **421**, 191 (2005).
[39] K. Ackerstaff *et al.* (OPAL Collaboration), Eur. Phys. J. C **7**, 571 (1999).
[40] B. Aubert *et al.* (*BABAR* Collaboration), Phys. Rev. D **77**, 092002 (2008).
[41] C. Patrignani *et al.* (Particle Data Group), Chin. Phys. C **40**, 100001 (2016).
[42] M. Bruno, M. D. Brida, P. Fritzsch, T. Korzec, A. Ramos, S. Schaefer, H. Simma, S. Sint, and R. Sommer (ALPHA Collaboration), Phys. Rev. Lett. **119**, 102001 (2017).
[43] M. D. Brida, P. Fritzsch, T. Korzec, A. Ramos, S. Sint, and R. Sommer (ALPHA Collaboration), Phys. Rev. Lett. **117**, 182001 (2016).
[44] C. Redmer (BESIII Collaboration), *Proceedings at Workshop on hadronic vacuum polarization contributions to muon g−2, KEK, Tsukuba* (2018); *Hadronic Cross Sections at BESIII*, https://kds.kek.jp/indico/event/26780/session/5/contribution/11/material/slides/0.pdf.
[45] S. Eidelman, *Proceedings at Radio MonteCarLOW Meeting, JGU, Mainz* (2017), *Generator for* $e^+e^- \to$ hadrons, https://agenda.infn.it/getFile.py/access?contribId=11&resId=0&materialId=slides&confId=13068.